# A Comparison of the Properties of Various Fused-Ring Quinones and Their Radical Anions Using Hartree−Fock and Hybrid Hartree−Fock/Density Functional Methods

**Anthony K. Grafton and Ralph A. Wheeler***

*Department of Chemistry and Biochemistry, University of Oklahoma, 620 Parrington Oval, Room 208, Norman, Oklahoma 73019*

*Received: May 1, 1997; In Final Form: June 25, 1997*[⊗]

The hybrid Hartree−Fock/density functional B3LYP has been used to predict a variety of properties of 1,4-naphthoquinone, 2-methyl-1,4-naphthoquinone, 2,3-dimethyl-1,4-naphthoquinone, and 9,10-anthraquinone, as well as their radical anions. Geometries and spin properties show good agreement with experiment. The calculated adiabatic electron affinities show excellent agreement with previously determined experimental values, where available. An electron affinity of 1.63 eV is predicted for 2,3-dimethyl-1,4-naphthoquinone. A complete analysis of the vibrational spectra of each neutral molecule is provided and compared with available experimental and previous theoretical results. In each case, the C═O antisymmetric stretching vibration is found to be slightly higher in frequency than the C═O symmetric stretch. The first full analysis of the vibrational spectra of each of the radical anions is presented, and a comparison is made with the spectra of the neutral molecules. It is found that B3LYP/6-31G(d) theory consistently overestimates vibrational frequencies by 4−5%, in agreement with previous tests, but also does an excellent job of predicting the correct relative ordering of vibrational modes. Unrestricted Hartree−Fock geometries and frequencies are also provided for comparison.

## 1. Introduction

The quinones and their one-electron reduced forms, or semiquinone anions, occupy a central place in electron transfer chemistry and biological energy conversion.[1−4] For example, quinones are known to play a crucial role in oxido reductases[5−12] and semiquinones are known intermediates in the actions of some antitumor drugs.[13] In photosynthesis, quinones act as primary and secondary electron acceptors, both in plant and bacterial photosynthetic reaction centers,[14−17] where semiquinone anions are known to be formed and remain stable for reasonably long times.[4] In the *Rhodopseudomonas viridis* reaction center, it is a fused-ring quinone, menaquinone, which occupies the primary quinone binding site, $Q_A$. Menaquinone (see Figure 1), or vitamin $K_2$, is made up of a 1,4-naphthoquinone head group with a methyl substituent at the 2 position and an isoprenoid chain of varying length at the 3 position. Various forms of vitamin K, with different alkyl substituents, occur elsewhere in nature. Some forms of vitamin K are known to be critical in the blood-clotting cascade[18,19] and in calcium homeostasis,[18,20,21] and the Rieske FeS center in certain bacteria uses a menaquinone pool, rather than plastoquinone or ubiquinone.[22−24] Simpler, but similar, compounds have been used as models of menaquinone in various theoretical and experimental studies to determine the function of the native quinone.[25−30] Some of these compounds include the parent 1,4-naphthoquinone (NQ), 2-methyl-1,4-naphthoquinone (2NQ, also known as vitamin $K_3$), and 2,3-dimethyl-1,4-naphthoquinone (23NQ). Various properties of these molecules, such as their fundamental vibrational frequencies[31−39] and their hyperfine interactions,[40−45] are used to infer information such as binding sites and protein interaction in the photosynthetic reaction center. A knowledge of the properties of the isolated molecules and their radical anions is therefore crucial for the interpretation of experimental results.[46]

For the simpler quinones, the structures have been investigated relatively thoroughly.[47] The structure of the parent 1,4-benzoquinone (*p*-benzoquinone, PBQ) has been determined experimentally both in the solid[48] and gas phases,[49] and these studies have been supported by theoretical determinations using *ab initio* and density functional theory.[50−52] The structure of the radical anion of PBQ (1,4-benzosemiquinone, $PBQ^{\bullet-}$), while not determined experimentally, has been predicted computationally using numerous techniques.[52−57] The current studies all agree that upon one-electron reduction the C═O and C═C bonds of PBQ lengthen while the C−C bonds shorten, with the overall effect of making the ring structure of $PBQ^{\bullet-}$ more benzenoid. These changes in bonding are consistent with the odd electron entering a molecular orbital which is antibonding with respect to C═O and C═C bonds and bonding with respect to C−C single bonds.[58]

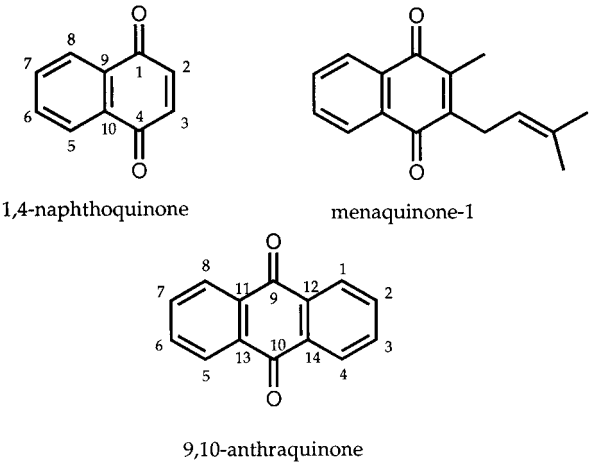


**Figure 1.** The structures of 1,4-naphthoquinone (NQ), menaquinone-1 (MQ-1), and 9,10-anthraquinone (AQ).

The structures of the larger, more biologically important quinones such as menaquinone (MQ), plastoquinone (PQ), and ubiquinone (UQ) and their radical anions have received theoretical attention only recently,[55−57,59,99] and no experimental structures of the isolated molecules are currently available.

[⊗] Abstract published in *Advance ACS Abstracts,* September 1, 1997.

S1089-5639(97)01481-3 CCC: $14.00 

**TABLE 1: Calculated Bond Distances (Å) and Bond Angles (deg) of 1,4-Naphthoquinone, 2-Methyl-1,4-naphthoquinone, and 2,3-Dimethyl-1,4-naphthoquinone**

| | NQ | | | | 2NQ | | 23NQ | |
|---|---|---|---|---|---|---|---|---|
| | expt.[65] (X-ray) | RHF[85] | BP86[84] | B3LYP | RHF[85] | B3LYP | expt.[66] (X-ray) | B3LYP |
| C1═O[a] | 1.22 | 1.222 | 1.239 | 1.226 | 1.223 | 1.226 | 1.24 | 1.227 |
| C4═O | 1.21 | 1.222 | 1.239 | 1.226 | 1.224 | 1.227 | 1.23 | 1.227 |
| C2−C3 | 1.31 | 1.327 | 1.356 | 1.344 | 1.332 | 1.350 | 1.34 | 1.358 |
| C9−C10 | 1.39 | 1.397 | 1.418 | 1.409 | 1.395 | 1.407 | 1.40 | 1.404 |
| C6−C7 | 1.37 | 1.388 | 1.408 | 1.399 | 1.389 | 1.399 | 1.37 | 1.399 |
| C1−C2 | 1.48 | 1.477 | 1.488 | 1.485 | 1.490 | 1.501 | 1.47 | 1.495 |
| C3−C4 | 1.45 | 1.477 | 1.488 | 1.485 | 1.473 | 1.478 | 1.45 | 1.495 |
| C1−C9 | 1.43 | 1.483 | 1.496 | 1.492 | 1.483 | 1.491 | 1.45 | 1.489 |
| C4−C10 | 1.46 | 1.483 | 1.496 | 1.492 | 1.482 | 1.490 | 1.49 | 1.489 |
| C8−C9 | 1.39 | 1.388 | 1.406 | 1.398 | 1.388 | 1.399 | 1.40 | 1.398 |
| C5−C10 | 1.36 | 1.388 | 1.406 | 1.398 | 1.388 | 1.397 | 1.39 | 1.398 |
| C5−C6 | 1.43 | 1.386 | 1.401 | 1.393 | 1.386 | 1.394 | 1.39 | 1.393 |
| C7−C8 | 1.41 | 1.386 | 1.401 | 1.393 | 1.386 | 1.393 | 1.39 | 1.393 |
| avg dev from expt | | 0.020 | 0.030 | 0.027 | | | | 0.015 |
| O−C1−C2 | 118.5 | | | 120.5 | | 120.6 | 119.0 | 120.8 |
| O−C4−C3 | 118 | | | 120.5 | | 120.6 | 120.0 | 120.8 |
| C2−C1−C9 | 121.5 | | 117.2 | 117.3 | | 118.2 | 121.5 | 118.4 |
| C3−C4−C10 | 123 | | 117.2 | 117.3 | | 117.4 | 120.8 | 118.4 |
| C1−C2−C3 | 120.5 | | 122.2 | 122.2 | | 119.6 | 119.7 | 121.2 |
| C4−C3−C2 | 117.5 | | 122.2 | 122.2 | | 124.0 | 120.7 | 121.2 |
| C1−C9−C8 | 123 | | 119.6 | 119.6 | | 119.4 | 121.0 | 119.7 |
| C4−C10−C5 | 123.5 | | 119.6 | 119.6 | | 119.9 | 120.2 | 119.7 |
| C1−C9−C10 | 118 | | 120.6 | 120.6 | | 120.8 | 119.5 | 120.3 |
| C4−C10−C9 | 117.5 | | 120.6 | 120.6 | | 120.0 | 117.7 | 120.3 |
| C7−C8−C9 | 121 | | 120.0 | 120.0 | | 120.0 | 117.5 | 119.9 |
| C6−C5−C10 | 121.5 | | 120.0 | 120.0 | | 119.9 | 118.2 | 119.9 |
| C5−C6−C7 | 118.5 | | 120.2 | 120.2 | | 120.1 | 119.7 | 120.2 |
| C8−C7−C6 | 119 | | 120.2 | 120.2 | | 120.2 | 123.2 | 120.2 |
| avg dev from expt | | | 2.9 | 2.9 | | | | 1.6 |

[a] Atom numbering is consistent with Figure 1.

However, low-resolution X-ray structures of the photosynthetic reaction centers of certain purple bacteria contain these molecules in their native protein environment,[17] and a recent study examined the conformation of the isoprenyl side chains.[41] There are experimental structures of some related quinones which may serve as models of the larger species. X-ray structures of 2-methyl-1,4-benzoquinone,[60] 2,3-dimethyl-PBQ, 2,5-dimethyl-PBQ,[61] 2,6-dimethyl-PBQ,[62] 2,3,5,6-tetramethyl-PBQ (duroquinone, DQ),[63] 2-methyl-5,6-methoxy-PBQ (UQ0),[64] 1,4-naphthoquinone (NQ),[65] 2,3-dimethyl-NQ (23NQ),[66] and 9,10-anthraquinone (AQ)[67,68] have been determined over the last 50 years. More recently, the gas-phase electron diffraction structures of PBQ,[49] DQ,[69] and AQ[70] were reported.

Considering the wide-ranging importance of quinones as biological electron acceptors, it somewhat surprising that the radical anions of the quinones have received much less attention. Of the semiquinone radical anions, only the simplest species, $PBQ^{\bullet-}$, has been studied extensively with theoretical methods. More information on the other semiquinone anions has recently begun to appear, but in some cases, such as the vitamin K analogues $NQ^{\bullet-}$, $2NQ^{\bullet-}$, and $23NQ^{\bullet-}$, a detailed comparison of their properties has yet to be performed.

Although the vibrational spectra of NQ and AQ have been studied relatively thoroughly both by experimental[71−82] and theoretical methods,[83−86] there is very little spectral data in the current literature for the radical anions of these molecules. Similarly, the vibrational spectra of 2NQ and 23NQ, both idealized model compounds for vitamin K, have been studied,[73,76,85,87,88] but a comprehensive analysis of the fundamental vibrational frequencies of these molecules and their radical anions has not yet been conducted. The vibrational spectrum of the most basic of the *p*-quinones, 1,4-benzoquinone, has been investigated by many methods. Many early experimental studies[77,89−92] concluded that the C═O stretching band of quinones, which is highly influenced by reduction[73,93] and therefore the most widely monitored in experimental studies, was seen as a doublet because of a Fermi resonance or some intermolecular interaction. Some work concluded that NQ exhibits only one C═O stretching frequency.[94] Recent theoretical studies indicate that there are actually two distinct fundamental C═O stretching vibrational frequencies of PBQ and NQ.

The ability to predict other properties of quinones accurately, such as the electron affinities,[95] aqueous one-electron reduction potentials,[96−98] and isotropic hyperfine coupling constants (hfccs),[55−57,59,99−101] has been reported only recently. The density functional and hybrid Hartree−Fock/density functional (HF/DF) methods have proven very useful in this area and have been shown to give reasonable hfccs for other organic $\pi$-radicals as well.[57,102−108] In this study, we present such a comparison of the electron affinities of NQ, 2NQ, 23NQ, and AQ, the spin densities and isotropic hyperfine coupling constants of the radical anions of these quinones, and the geometries and harmonic vibrational frequencies of both the quinones and semiquinone anions. We compare and contrast these properties to those previously determined for MQ[56] and discuss their importance in the interpretation of experimental results, including the question of Fermi resonance involving the C═O stretches of NQ. A detailed description of our methods and analysis techniques can be found in the Appendix.

## 2. Results and Discussion

**2.1. Geometries.** Table 1 compares the available experimentally determined geometries of NQ, 2NQ, and 23NQ with the predictions of *ab initio* MO and density functional theories. When compared to the solid-state X-ray diffraction structure, the RHF/6-31G method gives the best average reproduction of bond distances,[85] with the hybrid B3LYP/6-31G(d) method

**TABLE 2: Calculated Bond Distances (Å) and Bond Angles (deg) of the Radical Anions of 1,4-Naphthoquinone, 2-Methyl-1,4-naphthoquinone, and 2,3-Dimethyl-1,4-naphthoquinone**

| | $NQ^{\bullet-}$ | | | $2NQ^{\bullet-}$ | | | $23NQ^{\bullet-}$ | |
|---|---|---|---|---|---|---|---|---|
| | UHF[85] 6-31G | UHF 6-31G(d) | B3LYP 6-31G(d) | UHF[85] 6-31G | UHF 6-31G(d) | B3LYP 6-31G(d) | UHF 6-31G(d) | B3LYP 6-31G(d) |
| C1═O[a] | 1.276 | 1.241 | 1.264 | 1.278 | 1.244 | 1.266 | 1.242 | 1.265 |
| C4═O | 1.276 | 1.241 | 1.263 | 1.275 | 1.240 | 1.263 | 1.242 | 1.265 |
| C2−C3 | 1.371 | 1.372 | 1.381 | 1.373 | 1.375 | 1.385 | 1.381 | 1.392 |
| C9−C10 | 1.406 | 1.402 | 1.423 | 1.405 | 1.400 | 1.421 | 1.397 | 1.420 |
| C6−C7 | 1.405 | 1.404 | 1.410 | 1.406 | 1.404 | 1.410 | 1.405 | 1.411 |
| C1−C2 | 1.418 | 1.424 | 1.440 | 1.426 | 1.431 | 1.450 | 1.434 | 1.451 |
| C3−C4 | 1.418 | 1.424 | 1.440 | 1.420 | 1.423 | 1.437 | 1.434 | 1.451 |
| C1−C9 | 1.463 | 1.475 | 1.478 | 1.459 | 1.474 | 1.475 | 1.469 | 1.471 |
| C4−C10 | 1.463 | 1.475 | 1.478 | 1.460 | 1.473 | 1.477 | 1.469 | 1.471 |
| C8−C9 | 1.407 | 1.406 | 1.409 | 1.409 | 1.407 | 1.410 | 1.408 | 1.410 |
| C5−C10 | 1.407 | 1.406 | 1.409 | 1.408 | 1.406 | 1.409 | 1.408 | 1.410 |
| C5−C6 | 1.372 | 1.370 | 1.385 | 1.371 | 1.369 | 1.386 | 1.369 | 1.385 |
| C7−C8 | 1.372 | 1.370 | 1.385 | 1.371 | 1.370 | 1.386 | 1.369 | 1.385 |
| O−C1−C2 | | 123.5 | 123.5 | | 123.5 | 122.9 | 123.3 | 122.8 |
| O−C4−C3 | | 123.5 | 123.5 | | 123.5 | 123.1 | 123.3 | 122.8 |
| C2−C1−C9 | | 115.3 | 115.1 | | 116.1 | 116.0 | 116.4 | 116.3 |
| C3−C4−C10 | | 115.3 | 115.1 | | 115.3 | 115.2 | 116.4 | 116.3 |
| C1−C2−C3 | | 123.3 | 123.4 | | 121.5 | 121.4 | 122.4 | 122.4 |
| C4−C3−C2 | | 123.3 | 123.4 | | 124.6 | 124.7 | 122.4 | 122.4 |
| C1−C9−C8 | | 119.5 | 119.5 | | 119.3 | 119.4 | 119.6 | 119.7 |
| C4−C10−C5 | | 119.5 | 119.5 | | 119.8 | 119.8 | 119.6 | 119.7 |
| C1−C9−C10 | | 121.4 | 121.5 | | 121.7 | 121.7 | 121.2 | 121.2 |
| C4−C10−C9 | | 121.4 | 121.5 | | 120.9 | 121.0 | 121.2 | 121.2 |
| C7−C8−C9 | | 121.0 | 121.1 | | 120.9 | 121.1 | 120.9 | 121.0 |
| C6−C5−C10 | | 121.0 | 121.1 | | 120.9 | 121.0 | 120.9 | 121.0 |
| C5−C6−C7 | | 119.9 | 119.9 | | 119.8 | 119.8 | 119.9 | 119.9 |
| C8−C7−C6 | | 119.9 | 119.9 | | 120.0 | 119.9 | 119.9 | 119.9 |

[a] Atom numbering is consistent with Figure 1.

slightly better than the gradient-corrected pure density functional BP86/6-31G(d) method,[84] which are both slightly worse than the UHF/6-31G(d) method. It is worth noting that the X-ray structure is distinctly asymmetric, implying that the ubiquitous crystal packing forces may have significantly altered the structure from that of the gas phase. Unfortunately, the gas-phase structure of NQ, which would be the best basis of comparison for the methods, has not been determined. The UHF/6-31G(d) method does slightly better in reproducing X-ray bond distances in 23NQ, but not as well as B3LYP/6-31G(d), which has an average absolute deviation in bond distance of 0.015 Å. We are aware of no experimentally determined structure of 2NQ for comparison.

When comparing the structures of the quinones listed in Table 1 to each other, some trends are identifiable in both experiment and theory. All bonds except those directly involved with the 2 or 3 position methyl substitution remain virtually constant throughout the series, including the characteristic C═O and C2═C3 bonds. Bond angles also show little change across the series, except around the substituted positions. The fused ring maintains its benzene-like structure, even including the shared C9−C10 bond, with average bond lengths just under 1.40 Å. When comparing these structures to the previously described structure of MQ[56] (determined with the B3LYP/6-31G(d) method), it may be seen that the structure of the ring system of 23NQ is almost identical to that of MQ, having bond distances usually within 0.003 Å, which implies that the isoprenoid chain has the same effect on the local structure of the ring system as a methyl group.

Table 2 presents the calculated structures of the radical anions $NQ^{\bullet-}$, $2NQ^{\bullet-}$, and $23NQ^{\bullet-}$ as determined by the UHF/6-31G[85] and UHF/6-31G(d) molecular orbital based methods, as well as by the HF/DF B3LYP/6-31G(d) method. We are aware of no experimental determinations of the structures of these radical anions. Each method predicts a slight lengthening of the C2═C3 bond with further methyl substitution, as well as a small increase in the C−C bonds neighboring the substituted position. The C═O bond lengths remain virtually unchanged through the series for a particular method, but the UHF/6-31G method predicts a C═O bond distance approximately 0.01 Å longer than those predicted by B3LYP/6-31G(d), which, at about 1.265 Å, is about 0.02 Å greater in length than that predicted with the UHF/6-31G(d) method. This difference is not repeated in other bonds, implying that the inclusion of polarization functions in the basis set plays an important role in the prediction of open-shell properties of the C═O fragment of quinones. As with the neutral species, the structure of $23NQ^{\bullet-}$ is virtually identical to that of $MQ^{\bullet-}$.

A comparison of the structures of the neutral quinones in Table 1 with the associated semiquinones in Table 2 indicates that the primary changes in bonding upon one-electron reduction are centered in the quinonoidal ring. C═O and C2═C3 bond lengths increase by about 0.04 Å, regardless of the method, while C1−C2 and C3−C4 bond lengths decrease by almost the same amount. The shared C9−C10 bond increases in length by about 0.01 Å, as do the adjacent C8−C9 and C5−C10 bonds and the more distant C6−C7 bond, while the other two fused ring C−C bonds decrease in length by almost the same amount. These changes in bonding suggest that while the odd electron enters a molecular orbital very similar to that in the parent PBQ molecule, there is nevertheless a small contribution from the fused ring (see Figure 2).

When considering that the fused ring has an effect on the lowest unoccupied molecular orbital (LUMO) of the neutral molecule which is, although small, greater than the effect of two substituted methyl groups at the 2 and 3 positions, it is natural to examine the effect of changing these methyl carbons into members of a second fused ring, thus creating a larger $\pi$-system. Therefore we include in Table 3 a comparison of the calculated structures of 9,10-anthraquinone (AQ) and its

**TABLE 3: Calculated and Experimental Bond Distances (Å) and Bond Angles (deg) of 9,10-Anthraquinone and Its Radical Anion**

| | AQ | | | | | $AQ^{\bullet-}$ | |
|---|---|---|---|---|---|---|---|
| | expt[70] gas phase | expt[67] X-ray | UHF 6-31G(d) | BLYP[109] 6-31G(d) | B3LYP 6-31G(d) | UHF 6-31G(d) | B3LYP 6-31G(d) |
| C9═O[a] | 1.220 | 1.15 | 1.197 | 1.242 | 1.226 | 1.239 | 1.260 |
| C9−C11 | 1.499 | 1.50 | 1.493 | 1.501 | 1.492 | 1.454 | 1.465 |
| C11−C1 | 1.400 | 1.39 | 1.389 | 1.411 | 1.400 | 1.415 | 1.414 |
| C1−C2 | 1.400 | 1.39 | 1.382 | 1.402 | 1.392 | 1.363 | 1.382 |
| C2−C3 | 1.400 | 1.385 | 1.388 | 1.411 | 1.400 | 1.413 | 1.415 |
| C11−C12 | 1.400 | 1.395 | 1.393 | 1.421 | 1.408 | 1.409 | 1.427 |
| C1−H | 1.087 | | 1.072 | 1.092 | 1.085 | 1.074 | 1.086 |
| C2−H | 1.087 | | 1.075 | 1.094 | 1.086 | 1.078 | 1.089 |
| avg dev from gas-phase expt | | | 0.011 | 0.010 | 0.003 | | |
| O−C9−C11 | 121.3 | 121 | 121.2 | 121.3 | 121.3 | 122.0 | 122.0 |
| C11−C9−C14 | 117.4 | 117.5 | 117.7 | 117.5 | 117.5 | 116.0 | 116.0 |
| C9−C11−C12 | 121.3 | 120 | 121.2 | | 121.3 | 122.0 | 122.0 |
| C1−C11−C12 | 120.1 | 120 | 119.9 | 119.7 | 119.7 | 118.9 | 122.0 |
| C11−C1−C2 | 119.8 | 120.5 | 120.0 | 120.2 | 120.2 | 121.2 | 121.3 |
| C1−C2−C3 | 119.8 | 120.8 | 120.2 | | 120.1 | 120.0 | 119.9 |
| C11−C1−H | 120.1 | | 118.9 | | 118.3 | 117.6 | 117.0 |
| C1−C2−H | 120.1 | | 119.9 | 119.9 | 119.9 | 120.2 | 120.2 |
| avg dev from gas-phase expt | | | 0.3 | | 0.4 | | |

[a] Atom numbering is consistent with Figure 1.

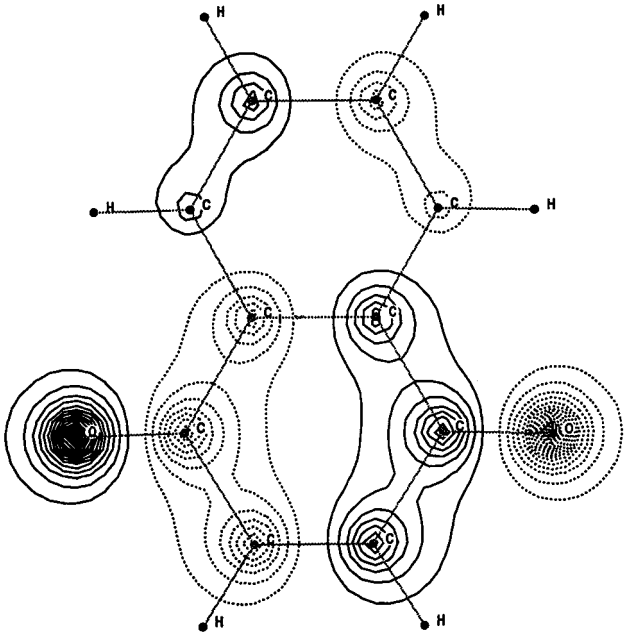

**Figure 2.** The LUMO of 1,4-naphthoquinone. The solid and dashed lines represent orbital lobes of opposite sign.

associated radical anion ($AQ^{\bullet-}$) with experiment. Here, B3LYP does an excellent job of reproducing bond distances and angles of the neutral, gas-phase molecule, with average absolute deviations of 0.003 Å and 0.4°, respectively, compared to the deviations in the UHF calculations of 0.011 Å and 0.3°. The structures of both the neutral and radical anion show excellent agreement with the analogous parameters of 23NQ, as do the trends in bonding changes upon one-electron reduction. Previous calculations by Ball[109] on AQ using the gradient-corrected pure density functional method BLYP (see Table 3) gave substantially poorer agreement with experiment than did B3LYP. BLYP overestimated the C═O bond lengths in particular by more than 0.02 Å, which is similar to the 0.019 Å overestimation of C═O bonds by the BP86 method in NQ.[84] These results indicate that hybrid HF/DF methods such as B3LYP are more reliable than gradient-corrected pure density functional methods such as BP86 and BLYP for predicting the structures of quinones.

**TABLE 4: Calculated (B3LYP/6-311G(d,p)) and Experimental Electron Affinities of Various Fused-Ring Quinones**

| molecule | calc EA (eV)[a] opt | calc EA (eV)[a] sgl pt | exptl EA[111,113] (eV) |
|---|---|---|---|
| 9,10-anthraquinone | 1.56 | 1.55 | 1.59 |
| 2,3-dimethyl-1,4-naphthoquinone | 1.63 | 1.63 | |
| menaquinone-1[45] | 1.68 | | |
| 2-methyl-1,4-naphthoquinone | 1.69 | 1.66 | 1.67−1.74 |
| 1,4-naphthoquinone | 1.75 | 1.75 | 1.73−1.81 |

[a] The first column of calculated electron affinities was obtained by fully optimizing each geometry with the 6-311G(d,p) basis set, while the second column was obtained by performing a single-point calculation with the larger basis on the optimized geometries from a 6-31G(d) calculation.

Because of the relatively slight changes in geometry when substituting one or two methyl groups or a fused ring, it is interesting to consider whether or not the similarities carry over to the other properties of the molecules. Therefore, we next discuss the calculated electron affinities of NQ, 2NQ, 23NQ, and AQ and compare these with the electron affinities of other quinones predicted previously. We will also discuss the spin properties of the radical anions of each of the molecules, as well as their harmonic vibrational frequencies.

**2.2. Electron Affinities.** Despite the importance of quinones as electron acceptors, relatively few of the electron affinities of the larger quinones have been determined experimentally. Attempts to predict the electron affinities of quinones with molecular orbital based HF methods have proven unsuccessful.[95,110] We have shown previously that the B3LYP method used with a reasonably large 6-311G(3d,p) or 6-311G(d,p) basis set can reliably predict the electron affinities of a variety of methylated and halogenated quinones to within about 0.05 eV.[95] Because the results with the 6-311G(d,p) basis set were nearly identical to those found using the larger 6-311G(3d,p) basis, the B3LYP/6-311G(d,p) method has been used to predict electron affinities of all three of the most biologically important quinones: plastoquinone,[59] ubiquinone,[55,99] and menaquinone.[56] None of these three electron affinities have been determined experimentally; however, those of some smaller, related quinones have been measured,[111−113] and we present in Table 4 a comparison of the calculated electron affinities of some of the fused-ring quinones with experiment.

**TABLE 5: Spin Densities and Hyperfine Coupling Constants (in Gauss) Determined for the Radical Anions of 1,4-Naphthoquinone, 2-Methyl-1,4-naphthoquinone, and 2,3-Dimethyl-1,4-naphthoquinone Using the B3LYP Method and a Variety of Basis Sets**

| | $NQ^{\bullet-}$ | | | | | | $2NQ^{\bullet-}$ | | | | | | $23NQ^{\bullet-}$ | | | |
|---|---|---|---|---|---|---|---|---|---|---|---|---|---|---|---|---|
| | 6-31G(d) | | 6-311G(d,p) | | [632\|41] | | 6-31G(d) | | 6-311G(d,p) | | [632\|41] | | 6-31G(d) | | 6-311G(d,p) | |
| | spin | hfcc | spin | hfcc | spin | hfcc | spin | hfcc | spin | hfcc | spin | hfcc | spin | hfcc | spin | hfcc |
| O1[a] | 0.26 | −8.3 | 0.25 | −5.3 | 0.24 | −6.9 | 0.25 | −8.4 | 0.25 | −5.4 | 0.24 | −6.6 | 0.26 | −8.4 | 0.25 | −5.3 |
| O4 | 0.26 | −8.3 | 0.25 | −5.3 | 0.24 | −6.9 | 0.25 | −8.1 | 0.24 | −5.1 | 0.23 | −6.7 | 0.26 | −8.4 | 0.25 | −5.3 |
| C1 | 0.07 | −0.4 | 0.07 | −3.6 | 0.09 | −2.6 | 0.08 | −1.0 | 0.08 | −3.1 | 0.08 | −2.0 | 0.08 | 0.5 | 0.07 | −3.0 |
| C2 | 0.12 | 2.9 | 0.12 | −0.2 | 0.11 | 0.6 | 0.10 | 4.0 | 0.11 | 0.0 | 0.11 | 0.8 | 0.10 | 2.5 | 0.11 | −0.2 |
| C3 | 0.12 | 2.9 | 0.12 | −0.2 | 0.11 | 0.6 | 0.11 | 2.8 | 0.12 | −0.4 | 0.11 | 0.1 | 0.10 | 2.5 | 0.11 | −0.2 |
| C4 | 0.07 | −0.4 | 0.07 | −3.6 | 0.09 | −2.6 | 0.06 | −0.3 | 0.06 | −3.6 | 0.10 | −2.8 | 0.08 | 0.5 | 0.07 | −3.0 |
| C5 | −0.01 | −0.9 | 0.00 | −1.1 | 0.00 | −1.1 | −0.01 | −0.8 | −0.01 | −1.3 | −0.01 | −1.3 | 0.00 | −0.9 | 0.00 | −1.2 |
| C6 | 0.03 | 0.9 | 0.03 | 0.3 | 0.02 | 0.4 | 0.03 | 0.7 | 0.03 | 0.5 | 0.03 | 0.7 | 0.03 | 0.9 | 0.03 | 0.3 |
| C7 | 0.03 | 0.9 | 0.03 | 0.3 | 0.02 | 0.4 | 0.02 | 0.9 | 0.02 | 0.1 | 0.02 | 0.2 | 0.03 | 0.9 | 0.03 | 0.3 |
| C8 | −0.01 | −0.9 | 0.00 | −1.1 | 0.00 | −1.1 | 0.00 | −1.0 | 0.00 | −0.9 | 0.00 | −1.0 | 0.00 | −0.9 | 0.00 | −1.2 |
| C9 | 0.05 | 0.5 | 0.05 | −1.0 | 0.04 | −0.7 | 0.04 | 0.5 | 0.04 | −1.3 | 0.04 | −1.0 | 0.05 | 0.5 | 0.05 | −1.0 |
| C10 | 0.05 | 0.5 | 0.05 | −1.0 | 0.04 | −0.7 | 0.06 | 0.3 | 0.06 | −0.7 | 0.05 | −0.3 | 0.05 | 0.5 | 0.05 | −1.0 |
| H2 | −0.01 | −3.3 | −0.01 | −3.0 | −0.01 | −2.9 | | | | | | | | | | |
| H3 | −0.01 | −3.3 | −0.01 | −3.0 | −0.01 | −2.9 | −0.01 | −3.3 | −0.01 | −2.9 | −0.01 | −2.6 | | | | |
| H5 | 0.00 | −0.1 | 0.00 | 0.0 | 0.00 | −0.1 | 0.00 | −0.1 | 0.00 | 0.1 | 0.00 | 0.0 | 0.00 | −0.1 | 0.00 | −0.1 |
| H6 | 0.00 | −0.8 | 0.00 | −0.7 | 0.00 | −0.7 | 0.00 | −0.7 | 0.00 | −0.8 | 0.00 | −0.9 | 0.00 | −0.8 | 0.00 | −0.7 |
| H7 | 0.00 | −0.8 | 0.00 | −0.7 | 0.00 | −0.7 | 0.00 | −0.8 | 0.00 | −0.6 | 0.00 | −0.6 | 0.00 | −0.8 | 0.00 | −0.7 |
| H8 | 0.00 | −0.1 | 0.00 | 0.0 | 0.00 | −0.1 | 0.00 | 0.0 | 0.00 | −0.2 | 0.00 | −0.2 | 0.00 | −0.1 | 0.00 | −0.1 |
| C2(Me2) | | | | | | | −0.01 | −2.1 | −0.01 | −1.9 | −0.01 | −1.7 | −0.01 | −1.52 | −0.01 | −1.7 |
| C3(Me3) | | | | | | | | | | | | | −0.01 | −1.52 | −0.01 | −1.7 |
| H(Me2 avg) | | | | | | | 0.00 | 2.3 | 0.00 | 2.3 | 0.00 | 2.1 | 0.00 | 2.3 | 0.00 | 2.5 |
| H(Me3 avg) | | | | | | | | | | | | | 0.00 | 2.3 | 0.00 | 2.5 |

[a] Atom numbering is consistent with Figure 1.

We tried two methods of predicting the electron affinities, described in detail in the Appendix. The first method involves a full optimization of both the neutral species and its radical anion at the B3LYP/6-311G(d,p) level (see the column labeled "opt." in Table 4). The second method, tested for computational efficiency, involved only single-point calculations at the B3LYP/6-311G(d,p) level on optimized structures from B3LYP/6-31G(d) calculations (column labeled "sgl. pt." in Table 4). In two cases, NQ and 23NQ, the electron affinity was unchanged from one method to another. In the other two cases, AQ and 2NQ, the electron affinity decreased by 0.01 and 0.03 eV, respectively, and in both cases moved away from experimental values.

Table 4 shows that the trend found previously of decreasing electron affinity with increased methyl substitution on the quinone is also displayed in the fused-ring quinones. Adding a fused ring to PBQ (with a calculated electron affinity of 1.85 eV[95]) to form NQ reduces the electron affinity to 1.75 eV, and adding another fused ring to form AQ decreases the electron affinity by a further 0.2 eV to 1.56 eV. This reflects the trend found in the experimental numbers. What is perhaps unusual is that the calculated electron affinity of MQ-1 (1.68 eV) is only 0.01 eV lower than that of 2NQ (1.69 eV) and 0.05 eV higher than the predicted value of 1.63 eV for 23NQ. While the calculated electron affinities of 2NQ, MQ, and 23NQ are essentially equal within the error of the calculation (0.05 eV), we note that our previous study found that a change of the isoprenoid chain-terminal methyl groups on MQ-1 into hydrogens for computational efficiency actually raised the electron affinity to 1.73eV. These differences seem to imply that although the isoprenoid chain has the same structural effect on the ring as a methyl group (as discussed previously in section 2.1), its electronic effect is different, perhaps owing to some long-range "communication" between the double bond in the chain with the ring system. Considering that most naturally occurring forms of menaquinone have four or nine isoprenoid chain units and that the conformations of substituents may play a role in determining the electron affinity,[114] it may be interesting to explore the effects of lengthening the chain on the electron affinity.

**TABLE 6: Spin Densities and Hyperfine Coupling Constants (in Gauss) Determined for the Radical Anion of 9,10-Anthraquinone Using the B3LYP Method and Two Basis Sets**

| | $AQ^{\bullet-}$ | | | |
|---|---|---|---|---|
| | 6-31G(d) | | 6-311G(d,p) | |
| | spin | hfcc | spin | hfcc |
| O9[a] | 0.23 | −7.5 | 0.22 | −4.8 |
| C1 | −0.01 | −1.2 | −0.01 | −1.5 |
| C2 | 0.04 | 1.4 | 0.04 | 0.4 |
| C9 | 0.08 | 0.8 | 0.07 | −2.6 |
| C11 | 0.07 | 0.3 | 0.07 | −0.7 |
| H1 | 0.00 | 0.0 | 0.00 | 0.0 |
| H2 | 0.00 | −1.1 | 0.00 | −1.0 |

[a] Atom numbering is consistent with Figure 1.

**2.3. Spin Properties.** It is possible to study the electron transfer to a quinone and its hydrogen bonding environment *in vivo* for biological systems such as the photosynthetic reaction center using electron paramagnetic resonance experiments. Such studies have been performed to investigate the environment of both $Q_A$ and $Q_B$ in the photosynthetic reaction center of *Rhodobacter sphaeroides* and photosystem II. The information gathered in these studies provides important information on the orientation and close contacts of the quinone radicals.

In order to interpret these experiments, it would be helpful to have information on the free molecule as a basis for comparison to accurately determine the effects of the protein environment. We present calculated spin density distributions and isotropic hyperfine coupling constants (hfccs) for the heavy atoms and protons of $NQ^{\bullet-}$, $2NQ^{\bullet-}$, and $23NQ^{\bullet-}$ (Table 5) as well as those determined for $AQ^{\bullet-}$ (Table 6). These properties were determined using the B3LYP method and, where possible, three basis sets. The smaller 6-31G(d) basis set has been shown to give reasonable agreement with experiment when used with the B3LYP method.[57,103−105,115] In addition, we also employed a basis set developed by Chipman[116,117] designed specifically to reproduce spin properties in higher level calculations. This basis set, denoted [632|41], includes more diffuse and polarization functions on heavy atoms, as well as a tighter s-function

on hydrogens. The hfccs are proportional to the spin density at the nucleus, and calculating them accurately may provide a more stringent test of the methods than spin densities derived from population analysis.

Experiments on $NQ^{\bullet-}$ in various solvents[27,118,119] have given magnitudes of the H2 and H3 hfccs which range from 3.22 to 3.32, in excellent agreement with our calculated values of 2.9−3.3. For the H6 and H7 protons, our calculations predict hfcc magnitudes of 0.7−0.8, which is in reasonable agreement with the experimental range 0.57−0.655. The H5 and H8 protons show the smallest hfcc magnitudes, with experimental values ranging from 0.26 to 0.57, as compared to our calculated magnitudes of 0.1. The experimental ordering of H2 ≫ H6 > H8 is thus correctly reproduced by our calculations. Good agreement between experiment[27,118,119] and theory was also found for $23NQ^{\bullet-}$ and $MQ^{\bullet-}$.[56] In the case of the asymmetrically substituted $2NQ^{\bullet-}$, the results are more ambiguous since the experimental magnitudes of the H5, H6, H7, and H8 proton hfccs were found to be equal in some solvents. We are aware of no experimentally determined hfccs for the heavy atoms of these menaquinone analogues. Our calculations are also in agreement with previous experimental results that substitution of alkyl groups has little effect on the spin density distribution.[118] The results presented here also demonstrate significant differences in the hfccs obtained with the smaller 6-31G(d) basis set versus those obtained with the two larger basis sets.

For the radical anion of 9,10-anthraquinone, $AQ^{\bullet-}$, Table 6 gives a list of the spin densities and hfccs determined with the B3LYP method and the 6-31G(d) and 6-311G(d,p) basis sets. Here, as in the cases discussed earlier, basis set size has little effect on spin densities but a marked effect on the magnitudes and signs of the hfccs. The $^{17}O$ hfcc calculated with the 6-31G(d) basis set (−7.5 G) shows better agreement with the experimental value of 7.53 G[120] than does that calculated with the larger 6-311G(d,p) basis set (−4.8 G). Experimental values[121−126] of the proton hfcc at the 1 position range from 0.35 to 0.550 G, while those of the 2 position range from 0.93 to 0.97 G. Here, our calculated hfccs reproduce only the relative ordering of the proton hfccs: the magnitude of the calculated hfcc for the 2 position (−1.1) agrees well with the experimental values, but the B3LYP method predicts a hfcc of 0.0 G for the 1 position. Other theoretical methods have been used to determine hfccs for $AQ^{\bullet-}$, but without greater success.[127] To our knowledge, there are no $^{13}C$ hfccs available for $AQ^{\bullet-}$.

From the data in Table 5, it is clear that spin density shows little basis set dependence. Indeed, even the replacement of a hydrogen with a methyl group has little effect on spin distribution, which is not surprising since the odd electron is entering a $\pi$-type molecular orbital. Hyperfine coupling constants show a much larger dependence on the choice of basis set. Values of the oxygen coupling constant are consistently about 20% smaller in magnitude when using the Chipman basis instead of the 6-31G(d) basis and smaller still using the 6-311G(d,p) basis. It is possible that adding diffuse functions delocalizes too much of the spin away from the nucleus.[100] The hfccs of the C1 and C4 carbons each increase in magnitude with the larger [632|41] basis, but keep the same sign, while the 6-311G(d,p) basis set gives a greater increase in magnitude. The C2 and C3 carbons' hfccs tend to decrease in magnitude, changing sign for the 6-311G(d,p) basis, while the C9 and C10 carbons, shared by both the quinonoidal and fused rings, tend to remain at about the same magnitude but change sign with both of the larger basis sets. The C5, C6, C7, and C8 carbons of the fused ring show only a slight change with the larger basis set, as do the ring and methyl protons. We have been unable to complete a successful calculation using the [632|41] basis set for either $23NQ^{\bullet-}$ and $AQ^{\bullet-}$, but we are currently exploring possible alternatives. It should be noted that the spin contamination (which may be an indicator of the accuracy of the calculation) of the wave functions used to determine the spin properties of the semiquinones, including anthraquinone, were quite low, with $\langle s^2 \rangle$ at about 0.76 before spin annihilation[128,129] and exactly 0.75, the expected analytical value, after.

**2.4. Vibrational Frequencies.** A complete listing of the vibrational modes and assignments determined with the B3LYP/6-31G(d) method for NQ and its radical anion is given in Table 7, along with the most complete previous experimental and theoretical assignments. For 2NQ, 23NQ, and AQ, only the modes in the spectroscopically important region 1800−1550 $cm^{-1}$ determined with the B3LYP/6-31G(d) method are listed in Table 8 along with available experimental data. A complete list of modes and assignments for each molecule and its radical anion determined using both the B3LYP/6-31G(d) and UHF/6-31G(d) methods, may be found in the Supporting Information.

**2.4.1. Neutral NQ.** For the neutral molecule NQ, we found all six C−H stretching modes from 3200 to 3226 $cm^{-1}$. The previous experimental studies found these modes in the range 3020−3085 $cm^{-1}$, indicating that the frequencies predicted with the HF/DF method are about 5% too high. UHF/6-31G(d) C−H stretching frequencies (after scaling by 0.8929) are found between 2999 and 3037 $cm^{-1}$. The B3LYP ordering of the vibrations in this region agrees exactly with that determined by Nonella[84] using the gradient-corrected pure DF BP86/6-31G(d,p) method, and is very similar to that found experimentally by Singh,[75] except that the two highest modes appear to be reversed. Pecile[71] also found an ordering of the two highest C−H stretching modes similar to that of Nonella, but also assigned the lowest $a_1$ mode and next-to-lowest $b_2$ mode in a reversed order. Of the C−H stretching modes identified by Girlando,[74] four were uncertain.

In the region 1550−1800 $cm^{-1}$, we identify six fundamental vibrations of the neutral molecule: two C═O stretches at 1757 and 1752 $cm^{-1}$ and three C−C stretches at 1679, 1649, and 1629 $cm^{-1}$ (see Figure 3). Of the C═O stretches, the B3LYP method predicts that the $b_2$ mode (antisymmetric stretch) is the higher frequency mode, with the $a_1$ mode (symmetric stretch) only 5 $cm^{-1}$ lower. This ordering is in agreement with the experimental work of Girlando, Pecile, and Balakrishnan,[85] as well as the theoretical assignments by Nonella. The theoretical assignments of Balakrishnan using the HF/6-31G method show the same ordering, with a much larger difference between the frequencies (1712 $cm^{-1}$ for the $a_1$ mode, and 1681 $cm^{-1}$ for the $b_2$ mode). Using the UHF/6-31G(d) method (Supporting Information, Table 1S), we find that these two modes are reversed with respect to experiment, with the symmetric stretch at 1783 $cm^{-1}$, and the antisymmetric stretch at 1769 $cm^{-1}$. Singh observed modes at 1678 $cm^{-1}$ and 1663 $cm^{-1}$ but assigned them to a Fermi resonance doublet, while Brown[76] found vibrational modes at 1674 and 1663 $cm^{-1}$, but was uncertain whether or not these were true fundamentals, the result of a Fermi resonance, or some intermolecular interaction.

With respect to the three C−C stretching modes of the neutral molecule in the range 1550−1800 $cm^{-1}$, both the B3LYP and UHF methods predict the C2═C3 stretch to be highest in frequency, at 1679 and 1646 $cm^{-1}$ respectively. Girlando, Pecile, and Singh identified this mode at 1607, 1605, and 1588 $cm^{-1}$, respectively, while Balakrishnan did not assign this mode experimentally. Nonella's density functional study found the C2═C3 stretching mode at 1614 $cm^{-1}$. The last two C−C stretches of NQ in this frequency range are localized primarily

**TABLE 7: A Comparison of Unscaled B3LYP/6-31G(d) Vibrational Frequencies of 1,4-Naphthoquinone (NQ) and Its Radical Anion (in Parentheses) with the Most Complete Previous Experimental and Theoretical Assignments**

| mode symmetry and description | B3LYP NQ (NQ$^{\bullet-}$) | Nonella[84] BP86/6-31G(d,p) | Balakrishnan[85] expt | Girlando[74] expt | Pecile[71] expt | Singh[75] expt |
|---|---|---|---|---|---|---|
| $a_1$ C−H str | 3226 (3200) | 3139 | | 3076 | 3073 | 3072 |
| $b_2$ C−H str | 3224 (3197) | 3136 | | 3076 | 3079 | 3085 |
| $a_1$ C−H str | 3218 (3167) | 3130 | | 3076 | 3059 | 3062 |
| $a_1$ C−H str | 3208 (3161) | 3125 | | 3059 | 3030 | 3037? |
| $b_2$ C−H str | 3200 (3144) | 3112 | | 3076 | 3063 | 3020 |
| $b_2$ C−H str | 3193 (3140) | 3111 | | 3059 | 3030? | 2970 |
| $b_2$ C═O asym str | 1757 (1577) | 1675 | 1667 (1515) | 1672 | 1675 | 1678 |
| $a_1$ C═O sym str | 1752 (1655) | 1665 | 1660 (1441) | 1662 | 1663 | 1663 |
| $a_1$ C2−C3 str | 1679 (1523) | 1614 | (1603) | 1607 | 1605 | 1588 |
| $b_2$ C−C str | 1649 (1653) | 1591 | 1599 | 1600 | 1590 | 1605 |
| $a_1$ C−C str | 1629 (1577) | 1573 | (1537) | 1566 | 1573 | 1565 |
| $a_1$ C−H bend | 1521 (1485) | 1462 | 1445 | 1460 | 1467 | 1453 |
| $b_2$ C−H bend | 1500 (1484) | 1446 | 1407 | 1432 | 1456 | 1380 |
| $b_2$ C−H bend | 1403 (1433) | 1350 | 1357 (1327) | 1370 | 1378 | 1335 |
| $a_1$ C−C str | 1379 (1372) | 1373 | 1323 | 1328 | 1330 | |
| $a_1$ C−C str | 1329 (1251) | 1288 | | 1296 | 1292 | 1300 |
| $b_2$ C−H bend | 1316 (1326) | 1265 | | 1296 | 1303 | 1235 |
| $b_2$ C−H bend | 1260 (1248) | 1213 | | 1224 | 1160 | 1220 |
| $a_1$ C−H bend | 1196 (1182) | 1155 | | 1157 | 1233 | 1150 |
| $a_1$ C−H bend | 1172 (1150) | 1126 | | 1142 | 1147 | 1120 |
| $b_2$ C−H bend | 1142 (1147) | 1102 | | 1116 | 1117 | |
| $a_1$ C−H bend | 1078 (1068) | 1039 | | 1053 | 1056 | 1050 |
| $b_2$ C−C−C bend | 1077 (1089) | 1039 | | 1087 | 1093 | 1018 |
| $a_1$ fused ring breathe | 1043 (1040) | 1012 | | 1012 | 1021 | |
| $a_2$ C−H wag | 1028 (939) | 983 | | | | |
| $a_2$ C−H wag | 1015 (980) | 970 | | | | 998 |
| $b_1$ C−H wag | 995 (965) | 954 | | | 986 | 980 |
| $a_2$ C−H wag | 924 (878) | 886 | | | | |
| $b_1$ C−H wag | 881 (838) | 849 | | | 865 | 914 |
| $a_2$ quinone ring chair | 810 (795) | 780 | | | | |
| $b_2$ C−C−C bend | 794 (808) | 769 | | 774 | | |
| $b_1$ C−H wag | 786 (772) | 753 | | | 774 | 780 |
| $b_2$ C−C−C bend | 765 (768) | 740 | | 758 | | |
| $a_1$ C−C−C bend | 706 (714) | 685 | | 693 | 692 | 690 |
| $a_2$ fused ring chair | 696 (669) | 671 | | | | |
| $b_1$ quinone ring boat | 614 (628) | 590 | | | 611 | 563 |
| $b_2$ C═O asym bend | 599 (603) | 578 | | 598 | | 450 |
| $a_1$ C−C−C bend | 556 (562) | 539 | | 553 | 559 | 540 |
| $a_2$ fused ring deform | 480 (485) | 458 | | | | 410 |
| $b_2$ C−C−C bend | 453 (468) | 437 | | 448 | 412 | |
| $a_1$ C−C−C bend | 452 (464) | 440 | | 448 | 451 | |
| $b_1$ fused ring boat | 421 (434) | 402 | | | 372 | 470 |
| $a_1$ C═O sym bend | 375 (365) | 360 | | 368 | | 370 |
| $a_2$ C═O chair wag | 273 (349) | 253 | | | | 258 |
| $b_2$ C−C−C bend | 268 (269) | 255 | | 266 | 267 | |
| $b_1$ butterfly tors | 188 (201) | 182 | | | | |
| $a_2$ ring-ring twist | 128 (144) | 121 | | | | 202 |
| $b_1$ C═O boat wag | 88 (117) | 90 | | | 100 | 85 |

on the fused ring (see Figure 3), with the $b_2$ mode (1649 cm$^{-1}$) higher than the $a_1$ mode (1629 cm$^{-1}$) according to the B3LYP method and the HF method (at 1603 and 1582 cm$^{-1}$, respectively). This is in excellent agreement with previous experimental and theoretical studies. As with the C−H stretching modes, the fundamental vibrations in the range 1550−1800 cm$^{-1}$ predicted by the B3LYP/6-31G(d) method are about 5% too high relative to experiment.

The vibrational spectra below 1550 cm$^{-1}$ and above 1000 cm$^{-1}$ consist primarily of C−H in-plane bending modes but also include three modes which are predominantly C−C stretches as well as one C−C−C bending mode. The ordering of the modes in this region as predicted by the B3LYP/6-31G(d) method agrees well with the previous experimental assignments with a few exceptions. The $a_1$ symmetry C−C stretch identified at 1329 cm$^{-1}$ is higher than the $b_2$ C−H bending mode at 1316 cm$^{-1}$. While this is in agreement with Nonella and Singh, it is reversed in relation to the assignments of Pecile, and Girlando found these two modes at the same frequency. Also, the $a_1$ C−H bend and $b_2$ C−C−C bend predicted at 1078 and 1077 cm$^{-1}$ appear to be reversed with respect to the experimental assignments of Girlando and Pecile but are in agreement with the work of Singh, while Nonella predicts them to be found at the same frequency. Pecile assigned the modes at 1233 and 1160 cm$^{-1}$ to $a_1$ and $b_2$ C−H bends, respectively, while all other experimental and theoretical results give reversed assignments, indicating the possibility that these modes were originally misassigned. Nonella, using a gradient-corrected pure density functional method, assigned the modes at 1373 and 1350 cm$^{-1}$ to an $a_1$ C−C stretch and a $b_2$ C−H bend, respectively, which is in disagreement with our results and the results of all previous experiments. Frequencies in this region are overestimated by the HF/DF method by 3−5% relative to experiment.

Modes with frequencies less than 1000 cm$^{-1}$ are primarily out-of-plane modes, and there are fewer experimental assignments with which to compare our calculated frequencies. All modes within this range are correctly ordered by the B3LYP/6-31G(d) method with respect to the assignments of Girlando and are ordered similarly to those of Nonella except in two cases.

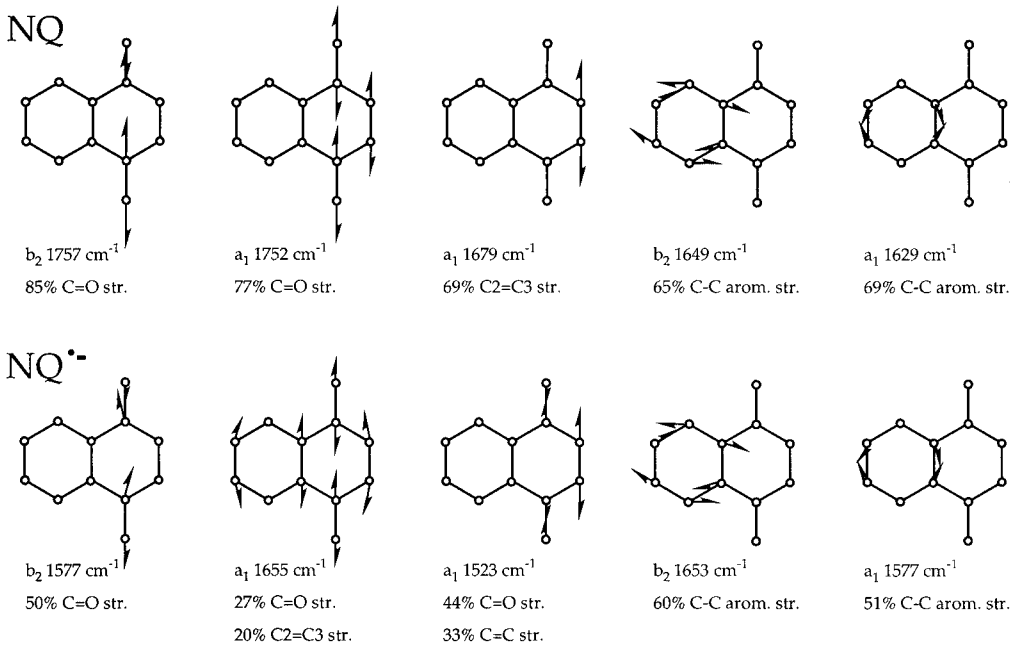


**Figure 3.** Atomic displacements and potential energy distributions of the five fundamental vibrational modes (determined with the B3LYP/6-31G(d) method) of naphthoquinone (NQ, top row) in the range 1800−1550 $cm^{-1}$ and the corresponding modes of naphthoquinone radical anion ($NQ^{\bullet-}$, bottom row). Hydrogen displacements have been omitted for clarity, and only major displacements of heavy atoms are shown.

The first case is the $a_2$ C═O chair wag and the $b_2$ C−C−C bend, predicted by B3LYP to be at 273 and 268 $cm^{-1}$, respectively, while Nonella found the order reversed at 253 and 255 $cm^{-1}$, respectively. The other disagreement is with the ordering of the $a_1$ and $b_2$ C−C−C bends predicted by B3LYP to be virtually identical at 453 and 452 $cm^{-1}$, which disagrees with the experimental ordering of Pecile and the theoretical ordering of Nonella, but is consistent with the experimental work of Girlando. The only conflict with the ordering of the modes by Singh in this region is a $b_2$ C═O bend predicted by B3LYP at 599 $cm^{-1}$ and the $a_1$ C−C−C bend at 556 $cm^{-1}$. Singh assigned these modes in reverse order, which conflicts both with our theoretical study as well as that of Nonella and with the experimental results of Girlando. The overestimation of frequencies in this range by the B3LYP/6-31G(d) method is generally about 3%, which is lower than that found at higher frequencies.

**2.4.2. $NQ^{\bullet-}$ Radical Anion.** The vibrations of the radical anions of naphthoquinone and its methylated derivatives have been only partially investigated with experimental and theoretical methods. To our knowledge, we provide here the first full vibrational analysis of $NQ^{\bullet-}$. Balakrishnan[85] recently reported several vibrational frequencies of $NQ^{\bullet-}$ and assigned them based on UHF calculations, and Clark[73] reported C═O stretching frequencies for both the radical anion and dianion of NQ.

Figure 3 is provided as a comparison of the atomic displacements and total energy distributions of the vibrations in the spectroscopically important range 1800−1550 $cm^{-1}$. Three of the assignments in this range are easy to make: the $b_2$ C═O antisymmetric stretch found at 1757 $cm^{-1}$ in NQ shifts downward to 1577 $cm^{-1}$ in the radical anion, and the $b_2$ and $a_1$ fused-ring C═C stretches at 1649 and 1629 $cm^{-1}$ in NQ shift to 1653 and 1577 $cm^{-1}$, respectively, in $NQ^{\bullet-}$. The two $a_1$ modes at 1752 and 1679 $cm^{-1}$ in NQ, however, are subject to a large degree of mixing, and the assignments become more difficult. When considering the total energy distributions only, it may be preferable to match the $NQ^{\bullet-}$ mode at 1523 $cm^{-1}$, which is predominantly the C═O stretch, with the NQ mode at 1752 $cm^{-1}$. However, considering that the phase of the C═O and C2═C3 stretching in the $NQ^{\bullet-}$ mode at 1523 $cm^{-1}$ is reversed with respect to the neutral mode, they become a questionable match. The radical anion mode at 1655 $cm^{-1}$ has the correct in-phase C═O and C2═C3 stretching to be a match for the NQ mode at 1752 $cm^{-1}$, but apparently has become mixed to a significant degree with the $a_1$ mode at 1577 $cm^{-1}$. Isotopic substitution of the oxygens (with $^{18}O$) shifts the three highest frequencies of the neutral molecule in this range downward by 32, 25, and 10 $cm^{-1}$, respectively, while shifting the last two neutral modes in this range, at 1649 and 1629 $cm^{-1}$, downward by only 1 $cm^{-1}$. The highest shift in the frequencies of the radical anion in this range upon $^{18}O$ substitution occurs for the mode at 1523 $cm^{-1}$, which shifts downward by 19 $cm^{-1}$. The next largest shift is for the $b_2$ mode at 1577 $cm^{-1}$, which shifts downward by 14 $cm^{-1}$, followed by the mode at 1655 $cm^{-1}$, which shifts downward by 6 $cm^{-1}$. The other two modes of $NQ^{\bullet-}$ at 1653 $cm^{-1}$ and the symmetric C═C stretch at 1577 $cm^{-1}$, shift downward by 2 and 4 $cm^{-1}$, respectively.

Although both the total energy distributions and isotopic substitution data tend to support the reverse, we choose to match the mode at 1655 $cm^{-1}$ in the radical anion with the C═O symmetric stretching mode at 1752 $cm^{-1}$ in NQ and the $NQ^{\bullet-}$ mode at 1523 $cm^{-1}$ with the C2═C3 stretching mode at 1679 $cm^{-1}$ in the neutral molecule because of the agreement in stretching phases. These assignments would suggest that the modes determined experimentally by Balakrishnan at 1603 and 1441 $cm^{-1}$ be reassigned to C2═C3 stretching and symmetric C═O stretching, respectively. However, if one chooses to dismiss the phase difference of the C═O and C2═C3 stretching found in the $a_1$ mode at 1523 $cm^{-1}$ of $NQ^{\bullet-}$ as an artifact of the theoretical method, then the isotopic substitution and total energy distribution calculations support the earlier assignments of Balakrishnan. In either case, assignment of vibrational modes in this region is difficult due to the high degree of mixing between the C═C and C═O stretches, and experimentally the spectrum is dominated by the very strong C═O stretching modes with nearby modes appearing only as shoulders.

Our Hartree−Fock calculations (Table 1S in the Supporting Information) using a 6-31G(d) basis set indicate that the $b_2$ C═O antisymmetric stretch in $NQ^{\bullet-}$ (at 1509 $cm^{-1}$) is lower than the $a_1$ C═O symmetric stretch (at 1622 $cm^{-1}$). Next highest in

**TABLE 8: A Comparison of the Spectroscopically Important Vibrational Modes Calculated Using the B3LYP/6-31G(d) Method for 2NQ, 23NQ, AQ, and Their Associated Radical Anions (in Parentheses) with Previous Experimental[a] and Theoretical Assignments**

2NQ (2-Methyl-1,4-naphthoquinone)

| mode | B3LYP | RHF[85] | Balakrishnan[85] expt | Clark[73] expt | Baucher[87] expt | Meyerson[77] expt | Brown[76] expt |
|---|---|---|---|---|---|---|---|
| $b_2$ C═O asym str | 1751 (1569) | 1707 (1379) | 1669 (1505) | 1661 (1505) | 1664 (1502) | 1673.0 | 1674 |
| $a_1$ C═O sym str | 1746 (1655) | 1673 (1424) | 1672 (1442) | | 1626 | 1665.5 | 1663 |
| $a_1$ C2−C3 str | 1694 (1549) | 1639 (1600) | 1624 (1605) | 1600 | 1596 | | |
| $b_2$ C−C arom str | 1649 (1649) | 1604 | 1599 (1539) | | | | |
| $a_1$ C−C arom str | 1632 (1580) | 1581 | | | | | |

23NQ (2,3-Dimethyl-1,4-naphthoquinone)

| mode | B3LYP | Breton[25] expt |
|---|---|---|
| $b_2$ C═O asym str | 1741 (1560) | 1670 |
| $a_1$ C═O sym str | 1735 (1639) | 1662 |
| $a_1$ C2−C3 str | 1674 (1542) | |
| $b_2$ C−C arom str | 1649 (1649) | |
| $a_1$ C−C arom str | 1633 (1570) | |

AQ (9,10-Anthraquinone)

| mode | B3LYP | Clark[73] expt | Stenman[81] expt | Girlando[74] expt | Gastilovich[82] expt | Gribov[86] expt | Singh[75] expt |
|---|---|---|---|---|---|---|---|
| $b_{1u}$ C═O asym str | 1756 (1558) | 1675 (1496) | | 1676 | | 1681 | 1670 |
| $a_g$ C═O sym str | 1747 (1645) | | 1666 | 1673 | 1677 | | 1675 |
| $b_{3g}$ C2−C3 str | 1650 (1642) | 1592 | | 1584 | 1625 | 1574 | 1625 |
| $b_{1u}$ C−C | 1646 (1655) | | | 1593 | | 1594 | 1585 |
| $a_g$ C−C | 1636 (1564) | | 1597 | 1603 | 1594 | | 1595 |
| $b_{2u}$ C−C | 1625 (1579) | | | 1582 | | | 1572 |

[a] Where experimental studies did not explicitly assign modes, assignments are suggested here. For a more complete discussion, see the text.

frequency are the $b_2$ and $a_1$ C═C fused-ring stretches at 1614 and 1531 $cm^{-1}$, respectively, with the C2═C3 stretch following at 1461 $cm^{-1}$. This is in agreement with the ordering described earlier for the B3LYP/6-31G(d) method.

With respect to the other vibrational frequencies of $NQ^{\bullet-}$, we find that, for the most part, the ordering is very similar to that of NQ. The C−H stretching modes of $NQ^{\bullet-}$, although all shifted downward by about 50 $cm^{-1}$, are found in exactly the same order as those of NQ. In the spectral region of 1000 to 1550 $cm^{-1}$, which is dominated primarily by C−H in-plane bending and C−C stretches, we find only two cases of mode reordering upon reduction. The $a_1$ C−C stretch and the $b_2$ C−H bend found at 1329 and 1316 $cm^{-1}$ in neutral NQ reverse position upon reduction and are found at 1251 and 1326 $cm^{-1}$, respectively. Also, the NQ $a_1$ C−H bending mode at 1078 $cm^{-1}$ and the C−C−C bend at 1077 $cm^{-1}$ are predicted to be reversed in ordering in $NQ^{\bullet-}$ at 1068 and 1089 $cm^{-1}$, respectively. Below 1000 $cm^{-1}$, several cases of reordering may be identified. The largest frequency shifts in this region upon reduction are found for the $a_2$ C═O chair wag, which shifts upward 76 $cm^{-1}$, or 28%, with respect to NQ, and the $b_1$ C═O boat wag, which shifts upward by 29 $cm^{-1}$, or 33%.

**2.4.3. 2NQ, 23NQ, and Their Radical Anions.** Because of limited experimental data and previous theoretical studies and because of the more extensive discussion of NQ and $NQ^{\bullet-}$ provided in previous sections of this report, we choose to limit our discussion of the vibrational modes of 2NQ, 23NQ, and their radical anions to the spectroscopically interesting region of 1550 to 1800 $cm^{-1}$. A complete description of all vibrational modes for each species obtained with the B3LYP/6-31G(d) and UHF/6-31G(d) methods may be found in the Supporting Information.

2NQ and its radical anion have been the subject of several experimental studies which focused especially on the C═O stretching frequencies. Table 8 shows the frequencies and assignments obtained in this work with the B3LYP method and compares them to the previous theoretical and experimental studies. Our calculations predict that the $b_2$ C═O antisymmetric stretch of 2NQ is slightly higher in frequency (by about 5 $cm^{-1}$) than the $a_1$ C═O symmetric stretch. Of the experimental studies by Baucher,[87] Meyerson,[77] and Brown,[76] none assigned these modes to "antisymmetric" or "symmetric" stretches, instead they generally favored the interpretation that the C═O splitting was the result of a Fermi resonance, or, in the case of Meyerson, that the splitting was the result of independent fundamental vibrations of either the proximal or distal (with respect to the antisymmetric substitution) carbonyl groups. Our work, as well as that of Balakrishnan, supports the notion that the carbonyl splitting results from two nearly degenerate fundamental vibrational modes, each involving both carbonyl groups vibrating either in-phase with each other (symmetric) or out-of-phase (antisymmetric). Our work with the B3LYP/6-31G(d) method and Balakrishnan's theoretical work using the RHF/6-31G method predict the antisymmetric C═O stretching mode to be higher in frequency, while the UHF/6-31G(d) method predicts the reverse.

As far as the overall ordering in this region of the spectrum for 2NQ, our calculated vibrational frequencies agree with experiment that the C═O stretching modes are highest, followed by the C2═C3 stretching mode, followed by the CC fused-ring stretching modes. This is the same calculated ordering as is found experimentally for NQ. When compared to experiment, the B3LYP/6-31G(d) modes are generally about 5% too high.

For the radical anion $2NQ^{\bullet-}$, there is much less experimental data. However, the data that are available (see Table 8) agrees that upon a one-electron reduction, at least one of the carbonyl stretching modes shifts downward by 9−10% to around 1505 $cm^{-1}$. This shift downward by 10% is reproduced well by the B3LYP/6-31G(d) (which, again, consistently overestimates absolute frequencies by about 5%) and UHF/6-31G(d) methods and less well (19%) by previous work[85] using the RHF/6-31G method.

As with $NQ^{\bullet-}$ (see section 2.4.2), we assign the $a_1$ C═O stretching mode of $2NQ^{\bullet-}$ to a frequency of 1655 $cm^{-1}$, followed by the CC fused-ring stretches at 1649 and 1580 $cm^{-1}$, followed in turn by the C2═C3 stretch at 1549 $cm^{-1}$. Unfortunately, there is not enough experimental work available to make a proper assessment of the B3LYP method for reproducing

the vibrational modes of $2NQ^{\bullet-}$ in this region, so the modes and assignments presented here represent predictions.

In the case of 23NQ and its radical anion $23NQ^{\bullet-}$, there are virtually no experimental studies on the vibrational modes with which to compare our results. Breton[25] assigned a mode at 1662 $cm^{-1}$ in 23NQ to a C═O vibration and identified, but did not assign, a shoulder at 1670 $cm^{-1}$. Because such a shoulder is a common feature of the C═O stretching frequencies, we suggest the assignment of this frequency to the $b_2$ C═O antisymmetric stretching mode, and the mode at 1662 $cm^{-1}$ to the symmetric C═O stretch. The overall ordering of the modes of 23NQ and $23NQ^{\bullet-}$ are predicted to be very similar to NQ and $NQ^{\bullet-}$. The UHF/6-31G(d) method again predicts the symmetric C═O stretch of 23NQ to be higher in frequency than the antisymmetric stretch, while both this method and the B3LYP/6-31G(d) method agree on the ordering of modes in the 1550−1800 $cm^{-1}$ range.

**2.4.4. AQ and $AQ^{\bullet-}$.** A thorough discussion of the vibrational modes of neutral AQ was recently reported by Ball,[109] so only a brief comparison of that work using the BLYP method with our results using the B3LYP method is given, followed by a comparison of the neutral and radical anion vibrations. A list of modes for both AQ and $AQ^{\bullet-}$ in found in the range 1550−1800 $cm^{-1}$ is given in Table 8, and a complete list of calculated vibrational modes and descriptions for both the B3LYP and UHF methods may be found in the Supporting Information (Tables 6S and 7S).

Our calculated vibrational frequency ordering agrees with that of Ball with only two minor exceptions. First, we find that the $b_{1u}$ C−C stretch (at 1193 $cm^{-1}$) and the $b_{2u}$ C−H bend (at 1192 $cm^{-1}$) are reversed with respect to the theoretical assignments of Ball and the experimental assignments of Pecile[130] but are in agreement with the experimental ordering found by Gazis[131] and Girlando.[74] Second, we find the $b_{3u}$ C−H wag mode to be higher in frequency (at 720 $cm^{-1}$) than the $a_g$ C−C−C bending mode (at 695 $cm^{-1}$), whereas Ball predicts them to have identical frequencies. In this case, our ordering agrees with the experimental work of Lehmann.[78] In both our work and Ball's, the ordering of the C═O stretches (with the antisymmetric stretch slightly higher than the symmetric stretch) agrees with the experimental work by Girlando and Lehmann but disagrees with the assignments of Singh.[75]

To our knowledge, experimental and theoretical studies of the radical anion $AQ^{\bullet-}$ are extremely limited. Only Clark[73] reports such information: a C═O stretching mode of $AQ^{\bullet-}$ at 1496 $cm^{-1}$. This 11% downward shift of the C═O vibration upon reduction is consistent with the other quinones described above, and the shift is accurately reproduced by our calculations, although both the neutral and anion C═O vibrational frequencies predicted with the B3LYP/6-31G(d) method are 5 and 4% too high, respectively. Our theoretical assignments also predict that the $a_g$ C═O stretching mode of AQ shifts downward upon reduction, but only by 6%, coming very close to the $b_{3g}$ and $b_{1u}$ C−C stretching modes at 1642 and 1655 $cm^{-1}$ in $AQ^{\bullet-}$. The $a_g$ and $b_{2u}$ modes found at 1636 and 1625 $cm^{-1}$ in AQ are predicted to shift downward by 4 and 3%, respectively, in the radical anion $AQ^{\bullet-}$.

## 3. Conclusions

We have presented the first full comparison, either experimental or theoretical, of the properties of 1,4-naphthoquinone (NQ), 2-methyl-1,4-naphthoquinone (2NQ), 2,3-dimethyl-1,4-naphthoquinone (23NQ), and 9,10-anthraquinone (AQ) and their radical anions. We have demonstrated that the geometries of the neutral molecules predicted with the B3LYP/6-31G(d) HF/DF method are consistently closer to experiment than those predicted using gradient-corrected pure density functional methods such as BLYP or BP86. On the basis of this knowledge, we offer predictions of the geometries of the radical anions of each of the species under investigation. This work also contains the first estimate of the electron affinity of 23NQ (1.63 eV), and demonstrates that the B3LYP/6-311G(d,p) method can reliably predict the electron affinities of other fused-ring quinones with respect to experiment. Our results also indicate that a full optimization at the B3LYP/6-311G(d,p) level of theory provides slightly better electron affinities than single-point calculations done at this level on B3LYP/6-31G(d) optimized geometries.

We have also shown that the B3LYP method, when used in combination with a 6-31G(d) basis set, can provide qualitatively correct spin densities of the radical anions of fused-ring quinones. When using the larger [632|41] and 6-311G(d,p) basis sets, the spin densities change very little with respect to the smaller basis sets, but the isotropic hyperfine coupling constants, especially those of the heavy atoms, can change substantially. Because of the lack of experimental data, our results leave unanswered the question of whether or not a larger basis set (such as 6-311G(d,p) or [632|41]) is necessary to obtain reliable heavy atom hfccs, although recent work indicates that large basis sets which are not augmented in the core region actually give worse hfccs for semiquinones.[100]

Also, we provide the first complete analysis of the vibrational spectra of the radical anions $NQ^{\bullet-}$, $2NQ^{\bullet-}$, $23NQ^{\bullet-}$, and $AQ^{\bullet-}$. The B3LYP/6-31G(d) method has been demonstrated to provide frequencies which are uniformly 4−5% too high with respect to experimental data, in agreement with previous tests, but the ordering of the frequencies is generally excellent. Where data exists, the B3LYP/6-31G(d) method can accurately predict the changes in the vibrational spectra of the fused ring quinones upon one-electron reduction.

This work is reported to aid the interpretation of experimental data, especially work in the photosynthetic reaction centers involving the replacement of the native quinones with other species. It is also useful in demonstrating the ability of the HF/DF B3LYP method to predict a wide range of molecular properties of quinones and their radical anions.

**Acknowledgment.** The research described in this publication was made possible by support from the Division of Chemical Sciences, Office of Basic Energy Sciences, Office of Energy Research, U.S. Department of Energy and by supercomputer time grants from the NSF/MetaCenter Allocations Committee award number MCA96N019, the NSF/National Center for Supercomputing Applications at the University of Illinois Urbana-Champaign, and the NSF/Cornell Theory Center. The Cornell Theory Center receives major funding from the NSF and New York State. Additional funding comes from ARPA, the NIH, IBM Corp., and other members of the center's Corporate Research Institute. The authors are also grateful for supercomputer time at the University of Oklahoma made possible by support from IBM Corp., Silicon Graphics Inc., and the University of Oklahoma. A.K.G. thanks the Phillips Petroleum Foundation and the University of Oklahoma Department of Chemistry and Biochemistry for fellowship support.

**Supporting Information Available:** Full vibrational frequency assignments for NQ and $NQ^{\bullet-}$ using the UHF/6-31G(d) method and for 2NQ, 23NQ, and AQ and their radical anions using both the B3LYP/6-31G(d) and UHF/6-31G(d) methods (7 pages). Ordering information is given on any current masthead page.

## Appendix: Computational Methods

All quantum calculations were performed using the Gaussian94 quantum chemistry program package.[132] All optimizations were performed using Berny's optimization algorithm[133] in redundant internal coordinates. For the hybrid Hartree−Fock/density functional method, the three-parameter Becke3LYP method was used. The hybrid methods incorporate a weighted sum of Hartree−Fock, local density functional, and gradient-corrected density functional exchange and correlational energies, where the various weighting factors have been determined by an empirical fit to experimental heats of formation.[132,134] We chose to use the Becke3LYP (or B3LYP) method instead of the Becke3P86[135] method because of past successes with B3LYP in reproducing the structures and vibrational frequencies of a variety of quinones[50] and semiquinones, as well as the adiabatic electron affinities of neutral quinones[95] and isotropic hyperfine coupling constants of many semiquinones and other organic $\pi$-radicals.[103−105,115] The optimized geometries, force constants, and partial atomic charges (determined with the CHELPG[136] electrostatic potential fitting algorithm) have been used to reproduce aqueous one-electron potentials of a variety of methylated and halogenated quinones.[96,137] To our knowledge, no *ab initio* or density functional method has been used successfully for determining such a wide range of molecular properties. We also include the results and discussion of unrestricted Hartree−Fock[138] calculations for comparison.

All Hartree−Fock vibrational frequencies reported here were determined with the UHF/6-31G(d) method and have been scaled by 0.8929. For the B3LYP method, the frequencies reported here are *not* scaled. We have chosen this procedure for two reasons. First, the scaling factor of 0.8929 for UHF/6-31G(d) frequencies is widely accepted.[139−143] Second, the HF/DF methods are relatively new and have not been subjected to the same extensive tests as have HF methods. Although a recent study[143] recommends a scaling factor of approximately 0.95 for B3LYP/6-31G(d) frequencies, other work suggests the use of multiple scaling factors for different mode types.[144,145] Because there is no general agreement on the degree of systematic overestimation of vibrational frequencies by HF/DF methods, we choose not to scale the frequencies reported here. We do, however, report the average percent deviation from experiment, where available, so that the reader may determine for himself what scaling factor, if any, should be applied.

All frequencies were assigned using a combination of total energy distributions,[146] graphical animation, and atomic displacement vector analysis. The total energy distributions were performed using the GAMESS[147] quantum chemistry program, using a set of internal coordinates consistent with the methodology of Boatz and Gordon.[148] Animation of the vibrational modes was accomplished using the program XMOL.[149] The descriptions of the modes reported here only include the major contributions.

Adiabatic electron affinities were determined using the B3LYP/6-311G(d,p) method which has been shown to give reliable electron affinities (to within 0.05 eV) for a variety of quinones.[95] This method has been used to predict electron affinities for all three of the biologically most important quinones: plastoquinone,[59] ubiquinone,[55,99] and menaquinone.[56] In all these previous studies, each molecule and its radical anion were fully optimized using the B3LYP/6-311G(d,p) method, and an electron affinity was determined by taking the difference in total energy between each species and its respective radical anion. We perform the same procedure here, but, because we are also interested in determining the most computationally efficient means of predicting electron affinities, we also include the results of a second procedure. In this new procedure, the optimized structures of each molecule and its radical anion were taken from B3LYP/6-31G(d) method, and single-point calculations were performed on these geometries with the larger 6-311G(d,p) basis set. The results of both procedures in determining electron affinities are presented here.

Spin densities and isotropic hyperfine coupling constants are reported for each atom in $NQ^{\bullet-}$, $2NQ^{\bullet-}$, $23NQ^{\bullet-}$, and $AQ^{\bullet-}$. They were determined using the B3LYP method and the 6-31G(d) and 6-311G(d,p) basis sets. Additionally, we also tested the Chipman diffuse-plus-polarization basis set[116,117] (also known as the [632|41] basis), which was designed to reproduce the spin properties in higher level calculations. With the [632|41] basis set, we performed only single-point calculations on the geometries obtained from the full optimizations using the B3LYP/6-311G(d,p) method. We encountered some difficulty achieving SCF convergence, and for $23NQ^{\bullet-}$ and $AQ^{\bullet-}$ were unable to perform a successful calculation.

Spin densities were determined using the Mulliken population analysis method, and are therefore only qualitatively correct. However, it has been demonstrated that the agreement with experimentally derived spin densities is reasonable for various organic $\pi$-radicals. Isotropic hyperfine coupling constants, which are dependent directly on the spin density value at the atomic nucleus, were determined directly from the Fermi contact terms, which are calculated by Gaussian94. The hfccs are related to the Fermi contact term, $\rho$(N), by the following equation[150,151]

$$a_o = [(8\pi/3)gg_N\beta\beta_N]\rho(N) \quad (1)$$

where $a_o$ is the hfcc (in Gauss), $g$ is the electronic $g$ factor, $\beta$ is the electronic Bohr magneton, and $g_N$ and $\beta_N$ are the analogous values for nucleus N. The terms in square brackets can be reduced to a single factor (in units of Gauss) for each type of nucleus: 1595 for $^1$H, 401.0 for $^{13}$C, and −216.2 for $^{17}$O.

## References and Notes

(1) Crofts, A. R.; Wraight, C. A. *Biochim. Biophys. Acta* **1983**, *726*, 149−185.
(2) Morton, R. A. *Biochemistry of Quinones*; Academic Press: New York, 1965.
(3) Robinson, H. H.; Crofts, A. R. *FEBS Lett.* **1983**, *153*, 221−226.
(4) *Function of Quinones in Energy Conserving Systems*; Trumpower, B. L., Ed.; Academic Press: New York, 1982.
(5) Smirnova, I. A.; Hägerhäll, C.; Konstantinov, A. A.; Hederstedt, L. *FEBS Lett.* **1995**, *359*, 23−26.
(6) Ferber, D. M.; Moy, B.; Maier, R. J. *Biochim. Biophys. Acta* **1995**, *1229*, 334−346.
(7) Prince, R. C.; Halbert, T. R.; Upton, T. H. In *Advances in Membrane Biochemistry and Bioenergetics*; Kim, C. H., Tedeshi, H., Diwan, J. J., Salerno, J. C., Eds.; Plenum: New York, 1988; pp 469−478.
(8) Reynolds, C. A.; King, P. M.; Richards, W. G. *Nature* **1988**, *334*, 80−82.
(9) O'Brian, M. R.; Maier, R. J. *J. Bacteriol.* **1985**, *161*, 775−777.
(10) Houchins, J. P. *Biochim. Biophys. Acta* **1984**, *768*, 227−255.
(11) Henry, M. F.; Vignais, P. *Arch. Microbiol.* **1983**, *136*, 64−68.
(12) Bokranz, M.; Katz, J.; Schroder, I.; Roberton, A.; Kröger, A. *Arch. Microbiol.* **1983**, *135*, 36−41.
(13) Powis, G. *Free Rad. Biol. Med.* **1989**, *6*, 63.
(14) Michel, H.; Deisenhofer, J. *Biochemistry* **1988**, *27*, 1−7.
(15) Mattoo, A. K.; Marder, J. B.; Edelman, M. *Cell* **1989**, *56*, 241−246.
(16) Diner, B. A.; Petrouleas, V.; Wendoloski, J. J. *Physiol. Plant* **1991**, *81*, 423−436.
(17) Deisenhofer, J.; Epp, O.; Miki, K.; Huber, R.; Michel, H. *Nature* **1985**, *318*, 618−624.
(18) Houser, R. M.; Jones, J. P.; Fausto, A.; Gardner, E. J.; Lee, F. C.; Olson, R. E. *Fed. Proc.* **1976**, *35*, 1353−1356.
(19) Sadowski, J. A.; Esmon, C. T.; Suttie, J. W. *J. Biol. Chem.* **1976**, *251*, 2770−2775.
(20) Price, P. A.; Otsuka, A. S.; Foser, J. W.; Kristaponis, J.; Ranan, N. *Proc. Natl. Acad. Sci. U.S.A.* **1976**, *73*, 1447−1451.

(21) Lian, J. B.; Hauschka, P. V.; Gallop, P. M. *Fed. Proc.* **1978**, *37*, 2615−2620.
(22) Collins, M. D.; Jones, D. *Microbiol. Rev.* **1981**, *45*, 316−354.
(23) Kutoh, E.; Sone, N. *J. Biol. Chem.* **1988**, *263*, 9020−9026.
(24) Hiraishi, A. *Arch. Microbiol.* **1989**, *151*, 378−379.
(25) Breton, J.; Burie, J.; Boullais, C.; Berger, G.; Nabedryk, E. *Biochemistry* **1994**, *33*, 12405−12415.
(26) Morris, A. L.; Snyder, S. W.; Zhang, Y.; Tang, J.; Thurnauer, M. C.; Dutton, P. L.; Robertson, D. E.; Gunner, M. R. *J. Phys. Chem.* **1995**, *99*, 3854−3866.
(27) Burghaus, O.; Plato, M.; Rohrer, M.; Möbius, K.; MacMillan, F.; Lubitz, W. *J. Phys. Chem.* **1993**, *97*, 7639−7647.
(28) Iwaki, M.; Itoh, S. *Biochemistry* **1991**, *30*, 5347−5352.
(29) Itoh, S.; Iwaki, M. *Biochemistry* **1991**, *30*, 5340−5346.
(30) Biggins, J. *Biochemistry* **1990**, *29*, 7259−7264.
(31) Gerwert, K.; Hess, B.; Michel, H.; Buchanan, S. *FEBS Lett.* **1988**, *232*, 303−307.
(32) Berthomieu, C.; Nabedryk, E.; Mäntele, W.; Breton, J. *FEBS Lett.* **1990**, *269*, 363−367.
(33) Breton, J.; Thibodeau, D. L.; Berthomieu, C.; Mäntele, W.; Verméglio, A.; Nabedryk, E. *FEBS Lett.* **1991**, *278*, 257−260.
(34) Breton, J.; Berthomieu, C.; Thibodeau, D. L.; Nabedryk, E. *FEBS Lett.* **1991**, *288*, 109−113.
(35) Bauscher, M.; Leonhard, M.; Moss, D. A.; Mäntele, W. *Biochim. Biophys. Acta* **1993**, *1183*, 59−71.
(36) Mäntele, W. In *The Photosynthetic Reaction Center*; Deisenhofer, J., Norris, R. J., Eds.; Academic Press: San Diego, CA, 1993; Vol. II, pp 239−283.
(37) Mäntele, W. In *Anoxygenic Photosynthetic Bacteria*; Blankenship, R. E., Madigan, M. T., Bauer, C. E., Eds.; Kluwer Academic Press: Dordrecht, The Netherlands, 1995; Vol. 2, pp 627−647.
(38) Breton, J.; Burie, J.; Berthomieu, C.; Berger, G.; Nabedryk, E. *Biochemistry* **1994**, *33*, 4953−4965.
(39) Breton, J.; Burie, J.-R.; Berthomieu, C.; Thibodeau, D. L.; Andrianambinintsoa, S.; Dejonghe, D.; Berger, G.; Nabedryk, E. In *The Photosynthetic Bacterila Reaction Center II: Structure, Spectroscopy and Dynamics*; Breton, J., Verméglio, A., Eds.; Plenum Press: New York, 1992; pp 155.
(40) MacMillan, F.; Lendzian, F.; Lubitz, W. *Magn. Reson. Chem.* **1995**, *33*, S81−S93.
(41) Zheng, M.; Dismukes, G. C. *Biochemistry* **1996**, *35*, 8955−8963.
(42) Brink, J. S. v. d.; Hulsebosch, R. J.; Gast, P.; Hore, P. J.; Hoff, A. J. *Biochemistry* **1994**, *33*, 13668−13677.
(43) Hallahan, B. J.; Ruffle, S. V.; Bowden, S. J.; Nugent, J. H. A. *Biochim. Biophys. Acta* **1991**, *1059*, 181−188.
(44) Rigby, S. E. J.; Heathcote, P.; Evans, M. C.; Nugent, H. A. *Biochemistry* **1995**, *34*, 12075−12081.
(45) Deligiannakis, Y.; Boussac, A.; Rutherford, A. W. *Biochemistry* **1995**, *34*, 16030−16038.
(46) Burie, J.-R.; Nonella, M.; Nabedryk, E.; Tavan, P.; Breton, J. In *Fifth International Conference on the Spectroscopy of Biological Molecules*; Theophanides, T., Anastassopoulou, J., Fotopoulos, N., Eds.; Kluwer Academic Publishers: Dordrecht, The Netherlands, 1993; pp 27.
(47) Bernstein, J.; Cohen, M. D.; Leiserowitz, L. In *The Chemistry of the Quinonoid Compounds*; Patai, S., Ed.; Wiley-Interscience: London, 1974; pp 37−110.
(48) Trotter, J. *Acta. Crystallogr.* **1960**, *13*, 86−95.
(49) Hagen, K.; Hedberg, K. *J. Chem. Phys.* **1973**, *59*, 158−162.
(50) Boesch, S. E.; Wheeler, R. A. *J. Phys. Chem.* **1995**, *99*, 8125−8134.
(51) Liu, R.; Zhou, X.; Pulay, P. *J. Phys. Chem.* **1992**, *96*, 4255−4261.
(52) Chipman, D. M.; Prebenda, M. F. *J. Phys. Chem.* **1986**, *90*, 5557−5560.
(53) Zhao, X.; Imahori, H.; Zhan, C.; Sakata, Y.; Iwata, S.; Kitagawa, T. *J. Chem. Soc. A* **1997**, *101*, 622−631.
(54) Nonella, M.; Brändli, C. *J. Phys. Chem.* **1996**, *100*, 14549−14559.
(55) Boesch, S. E. M.S. Thesis, University of Oklahoma, 1996.
(56) Grafton, A. K.; Boesch, S. E.; Wheeler, R. A. *J. Mol. Struct. (THEOCHEM)* **1997**, *392*, 1−11.
(57) O'Malley, P. J.; Collins, S. J. *Chem. Phys. Lett.* **1996**, *259*, 296−300.
(58) Wheeler, R. A. *J. Phys. Chem.* **1993**, *97*, 1533−1537.
(59) Wise, K. E.; Grafton, A. K.; Wheeler, R. A. *J. Phys. Chem. A* **1997**, *101*, 1160−1165.
(60) Trommsdorff, H. P.; Bordeaux, D.; Mentzafos, D. *C. R. Acad. Sci. Paris* **1970**, *271C*, 45−48.
(61) Rabinovich, D.; Schmidt, G. M. J. *J. Chem. Soc.* **1967**, 2030−2040.
(62) Rabinovich, D.; Schmidt, G. M. J. *J. Chem. Soc. B* **1967**, 127−131.
(63) Rabinovich, D.; Schmidt, G. M. J.; Ubell, E. *J. Chem. Soc. B* **1967**, 131−139.
(64) Silverman, J.; Stam-Thole, I.; Stam, C. H. *Acta. Crystallogr.* **1971**, *B27*, 1846−1851.
(65) Gaultier, J.; Hauw, C. *Acta. Crystallogr.* **1965**, *18*, 179−183.
(66) Brenton-Lacombe, M. *Acta. Crystallogr.* **1967**, *23*, 1024−1031.
(67) Sen, S. N. *Ind. J. Phys.* **1948**, *22*, 347−378.
(68) Lonsdale, K.; Milledge, H. J.; El Sayed, K. *Acta. Crystallogr.* **1966**, *20*, 1−13.
(69) Schei, H.; Hagen, K.; Trætteberg, M. *J. Mol. Struct.* **1980**, *62*, 121−130.
(70) Ketkar, S. N.; Kelley, M.; Fink, M. *J. Mol. Struct.* **1981**, *77*, 127−138.
(71) Pecile, C.; Lunelli, B.; Busetti, V. *J. Chem. Soc. A* **1970**, *5*, 690−697.
(72) Miyazaki, Y.; Ito, M. *Bull. Chem. Soc. Jpn.* **1973**, *46*, 103−106.
(73) Clark, B. R.; Evans, D. H. *J. Electroanal. Chem.* **1976**, *69*, 181−194.
(74) Girlando, A.; Ragazzon, D.; Pecile, C. *Spectrochim. Acta* **1980**, *36A*, 1053−1058.
(75) Singh, S. N.; Singh, R. S. *Spectrochim. Acta* **1968**, *24A*, 1591−1597.
(76) Brown, T. L. *Spectrochim. Acta* **1962**, *18*, 1065−1071.
(77) Meyerson, M. L. *Spectrochim. Acta* **1985**, *41A*, 1263−1267.
(78) Lehmann, K. K.; Smolarek, J.; Khalil, O. S.; Goodman, L. *J. Phys. Chem.* **1979**, *83*, 1200.
(79) Murao, T.; Azumi, T. *J. Chem. Phys.* **1979**, *70*, 4460.
(80) Kolev, T. *J. Mol. Struct.* **1995**, *349*, 381−384.
(81) Stenman, F. *J. Chem. Phys.* **1969**, *51*, 3413−3414.
(82) Gastilovich, E. A.; Dement'ev, V. A.; Mishenina, K. A. *Z. Fiz. Khim.* **1981**, *55*, 78−81.
(83) Strokach, N. S.; Kainkova, T. V.; Shigorin, D. N. *Z. Fiz. Khim.* **1986**, *60*, 114−119.
(84) Nonella, M. *J. Mol. Struct. (THEOCHEM)* **1996**, *362*, 7−21.
(85) Balakrishnan, G.; Mohandas, P.; Umapathy, S. *J. Phys. Chem.* **1996**, *100*, 16472−16478.
(86) Gribov, L. A.; Zubkova, O. B.; Sigarev, A. A. *Z. Struk. Khim.* **1993**, *34*, 169−178.
(87) Bauscher, M.; Mäntele, W. *J. Phys. Chem.* **1992**, *96*, 11101−11108.
(88) Burie, J.; Boussac, A.; Boullais, C.; Berger, G.; Mattioli, T.; Mioskowski, C.; Nabedryk, E.; Breton, J. *J. Phys. Chem.* **1995**, *99*, 4059−4070.
(89) Yates, P.; Ardao, M. I.; Fieser, L. F. *J. Am. Chem. Soc.* **1956**, *78*, 650−652.
(90) Bagli, J. F. *J. Am. Chem. Soc.* **1962**, *84*, 177−180.
(91) Bagli, J. F. *J. Phys. Chem.* **1961**, *65*, 1052−1053.
(92) Flaig, W.; Salfeld, J. *Liebigs Ann. Chem.* **1959**, *626*, 215−224.
(93) Eargle, D. H. J. *J. Org. Chem.* **1974**, *39*, 1295.
(94) Smith, R. W. M.S. Thesis, University of Georgia, 1954.
(95) Boesch, S. E.; Grafton, A. K.; Wheeler, R. A. *J. Phys. Chem.* **1996**, *100*, 10083−10087.
(96) Raymond, K. S.; Grafton, A. K.; Wheeler, R. A. *J. Phys. Chem. B* **1997**, *101*, 623−631.
(97) Mallik, B.; Datta, S. N. *Int. J. Quantum Chem.* **1994**, *52*, 629−649.
(98) Reynolds, C. A. *Int. J. Quantum Chem.* **1995**, *56*, 677−687.
(99) Boesch, S. E.; Wheeler, R. A. *J. Phys. Chem. A* **1997**, *101*, 5799−5804.
(100) Boesch, S. E.; Wheeler, R. A. *J. Phys. Chem. A*, in press.
(101) Nonella, M. *J. Phys. Chem. B* **1997**, *101*, 1235−1246.
(102) Batra, R.; Giese, B.; Spichty, M.; Gescheidt, G.; Houk, K. N. *J. Phys. Chem.* **1996**, *100*, 18371−18379.
(103) Qin, Y.; Wheeler, R. A. *J. Phys. Chem.* **1996**, *100*, 10554−10563.
(104) Walden, S. E.; Wheeler, R. A. *J. Phys. Chem.* **1996**, *100*, 1530−1535.
(105) Walden, S. E.; Wheeler, R. A. *J. Chem. Soc., Perkin Trans. 2* **1996**, 2663−2672.
(106) Barone, V. *Theor. Chim. Acta* **1995**, *1995*, 113−128.
(107) Eriksson, L. A.; Malkin, V. G.; Malkina, O. L.; Salahub, D. R. *Int. J. Quantum Chem.* **1994**, *52*, 879−901.
(108) Eriksson, L. A.; Malkin, V. G.; Malkina, O. L.; Salahub, K. R. *J. Chem. Phys.* **1993**, *99*, 9756−9763.
(109) Ball, B.; Zhou, X.; Liu, R. *Spectrochim. Acta* **1996**, *52A*, 1803−1814.
(110) Almlöf, J. E.; Feyereisen, M. W.; Jozefiak, T. H.; Miller, L. L. *J. Am. Chem. Soc.* **1990**, *112*, 1206−1214.
(111) Heinis, T.; Chowdhury, S.; Scott, S. L.; Kebarle, P. *J. Am. Chem. Soc.* **1988**, *110*, 400−407.
(112) Kebarle, P.; Chowdhury, S. *Chem. Rev.* **1987**, *87*, 513−534.
(113) Fukuda, E. K.; Jr., R. T. M. *J. Am. Chem. Soc.* **1985**, *107*, 2291−2296.
(114) Robinson, H. H.; Kahn, S. D. *J. Am. Chem. Soc.* **1990**, *112*, 4728−4731.
(115) Qin, Y.; Wheeler, R. A. *J. Chem. Phys.* **1995**, *102*, 1689−1698.
(116) Chipman, D. M. *Theor. Chim. Acta* **1989**, *76*, 73−84.
(117) Basis set was obtained from the Extensible Computational Chemistry Environment Basis Set Database, V., as developed and distributed by the Molecular Science Computing Facility, Environmental and Molecular Sciences Laboratory, which is part of the Pacific Northwest Laboratory, P.O. Box 999, Richland, Washington 99352, and funded by the U.S.

Department of Energy. The Pacific Northwest Laboratory is a multiprogram laboratory operated by Battelle Memorial Institute for the U.S. Department of Energy under contract DE-AC06-76RLO 1830. Contact David Feller, Karen Schuchardt, or Don Jones for further information.

(118) Das, M. R.; Connor, H. D.; Leniart, D. S.; Freed, J. H. *J. Am. Chem. Soc.* **1970**, *92*, 2258−2268.

(119) Fritch, J. M.; Tatwawadi, S. V.; Adams, R. N. *J. Phys. Chem.* **1967**, *71*, 338−342.

(120) Stevenson, G. R.; Wang, Z. Y.; Reiter, R. C.; Peters, S. J. *J. Am. Chem. Soc.* **1988**, *110*, 6581−6582.

(121) Baugh, P. J.; Phillips, G. O.; Arthur, J. C. J. *J. Phys. Chem.* **1966**, *70*, 3061−3069.

(122) Pederson, J. A. *J. Chem. Soc., Faraday Trans. I* **1988**, *84*, 3223−3231.

(123) Mäkelä, R.; Vuolle, M. *J. Chem. Soc., Faraday Trans.* **1990**, *86*, 2569−2573.

(124) Sieiro, C.; Sanchez, A.; Crouigneau, P. *Spectrochim. Acta* **1984**, *40A*, 453−456.

(125) Vuolle, M.; Mäkelä, R. *Magn. Reson. Chem.* **1992**, *30*, 987−991.

(126) Vuolle, M.; Mäkelä, R. *J. Chem. Soc., Faraday Trans. I* **1987**, 51−55.

(127) Eloranta, J.; Vatanen, V.; Grönroos, A.; Vuolle, M.; Mäkelä, R.; Heikkilä, H. *Magn. Reson. Chem.* **1996**, *34*, 898−902.

(128) Schlegel, H. B. *J. Chem. Phys.* **1986**, *84*, 4530−4534.

(129) Schlegel, H. B. *J. Phys. Chem.* **1988**, *92*, 3075−3078.

(130) Pecile, C.; Lunelli, B. *J. Chem. Phys.* **1967**, *46*, 2109.

(131) Gazis, E.; Heim, P. *Spectrochim. Acta* **1970**, *26A*, 497.

(132) Frisch, M. J.; Trucks, G. W.; Schlegel, H. B.; Gill, P. M. W.; Johnson, B. G.; Robb, M. A.; Cheeseman, J. R.; Keith, T.; Petersson, G. A.; Montgomery, J. A.; Raghavachari, K.; Al-Laham, M. A.; Zakrzewski, V. G.; Ortiz, J. V.; Foresman, J. B.; Cioslowski, J.; Stefanov, B. B.; Nanayakkara, A.; Challacombe, M.; Peng, C. Y.; Ayala, P. Y.; Chen, W.; Wong, M. W.; Andres, J. L.; Replogle, E. S.; Gomperts, R.; Martin, R. L.; Fox, D. J.; Binkley, J. S.; Defrees, D. J.; Baker, J.; Stewart, J. P.; Head-Gordon, M.; Gonzalez, C.; Pople, J. A. *GAUSSIAN94*; D.1 Gaussian, Inc.: Pittsburgh, PA, 1995.

(133) Schlegel, H. B. *J. Comput. Chem.* **1986**, *3*, 214−218.

(134) Stephens, P. J.; Devlin, F. J.; Chabalowski, C. F.; Frisch, M. J. *J. Phys. Chem.* **1994**, *98*, 11623−11627.

(135) Becke, A. D. *J. Chem. Phys.* **1993**, *98*, 1372−1377.

(136) Breneman, C. M.; Wiberg, K. B. *J. Comput. Chem.* **1990**, *11*, 361−373.

(137) Wheeler, R. A. *J. Am. Chem. Soc.* **1994**, *116*, 11048−11051.

(138) Hehre, W. J.; Radom, L.; Schleyer, P. v. R.; Pople, J. A. *Ab Initio Molecular Orbital Theory*; Wiley: New York, 1986.

(139) Pople, J. A.; Scott, A. P.; Wong, M. W.; Radom, L. *Isr. J. Chem.* **1993**, *33*, 345−350.

(140) Pople, J. A.; Head-Gordon, M.; Fox, D. J.; Raghavachari, K.; Curtiss, L. A. *J. Chem. Phys.* **1989**, *90*, 5622−5629.

(141) Curtiss, L. A.; Raghavachari, K.; Trucks, G. W.; Pople, J. A. *J. Chem. Phys.* **1991**, *94*, 7221−7230.

(142) Curtiss, L. A.; Carpenter, J. E.; Raghavachari, K.; Pople, J. A. *J. Chem. Phys.* **1992**, *96*, 9030−9034.

(143) Scott, A. P.; Radom, L. *J. Phys. Chem.* **1996**, *100*, 16502−16513.

(144) Rauhut, G.; Pulay, P. *J. Phys. Chem.* **1995**, *99*, 3093−3100.

(145) Rauhut, G.; Pulay, P. *J. Phys. Chem.* **1995**, *99*, 14572.

(146) Pulay, P.; Turok, F. *Acta Chim. Acad. Sci. Hung.* **1966**, *47*, 273−297.

(147) Schmidt, M. W.; Baldridge, K. K.; Boatz, J. A.; Jensen, J. H.; Koseki, S.; Gordon, M. S.; Nguyen, K. A.; Windus, T. L.; Elbert, S. T. *GAMESS*; 1990.

(148) Boatz, J. A.; Gordon, M. S. *J. Phys. Chem.* **1989**, *93*, 1819−1826.

(149) *XMOL*; 1.3.1 Minnesota Supercomputer Center, Inc.: Minneapolis, MN, 1993.

(150) Weltner W., Jr., *Magnetic Atoms and Molecules*; Scientific and Academic Editions: New York, NY, 1983.

(151) Drago, R. S. *Physical Methods for Chemists*, 2nd ed.; Saunders College Publishing: Ft. Worth, TX, 1992.